Distributed Detection in Massive MIMO Wireless Sensor Networks under Perfect and Imperfect CSI

Apoorva Chawla, *Student Member IEEE*, Adarsh Patel, *Member IEEE*, Aditya K. Jagannatham, *Member IEEE* and Pramod K. Varshney, *Life Fellow IEEE*

***Abstract*—This paper considers the problem of distributed detection for massive multiple-input multiple-output (MIMO) wireless sensor networks (WSNs). Neyman-Pearson (NP) criterion based fusion rules are developed at the fusion center (FC) that also incorporate the local probabilities of detection and false alarm of the constituent sensor nodes. Closed form expressions are obtained for the probabilities of detection and false alarm at the FC for various signaling schemes employed by the sensors. The fusion rules and analysis are extended to the scenario with imperfect CSI. Furthermore, signaling matrices are determined for the massive MIMO WSN to enhance detection performance. The asymptotic detection performance of the WSN is analyzed for the large antenna regime, which yields pertinent power scaling laws with respect to the number of antennas at the FC. Simulation results demonstrate the improved performance of the proposed schemes and also validate the theoretical findings.**

***Index Terms*— Distributed detection, massive multiple-input multiple-output (MIMO), wireless sensor networks (WSNs), Neyman-Pearson criterion.**

I. Introduction

Massive multiple-input multiple-output (MIMO) technology, also known as very large-scale MIMO, has attracted significant research interest as a potential solution to meet the ever-increasing demand for higher data rates in next generation wireless communication systems [2], [3]. A massive MIMO system employs a large antenna array comprising of hundreds of antennas at the base station (BS) to simultaneously serve a large number of users utilizing the same time-frequency resources [4], thereby leading to a significant increase in the spectral efficiency. Additionally, one can leverage simplified linear signal processing techniques at the massive MIMO base station [5] without compromising on the spectral efficiency, thus making them attractive for practical implementation. Moreover, it facilitates a reduction in the transmit power of the users, thereby simplifying hardware design [6]. As a result, there has been a growing interest in incorporating massive MIMO technology in wireless sensor networks (WSNs), which have been extensively deployed for sensing and surveillance applications because of their robustness to faults, cost effectiveness and flexibility of deployment [7], [8]. Due to the stringent power and bandwidth constraints in a WSN, the sensor nodes generally compress their observations in the form of one-bit local decisions prior to transmission to the fusion center (FC) [9], [10] for distributed detection [11], [12]. The local decisions are subsequently processed by the FC to arrive at a global decision regarding the event of interest. A brief review of the existing research in the area of distributed detection and its extension to WSNs employing massive antenna arrays is presented next.

This work was presented in part at the Eighty Eighth IEEE Vehicular Technology Conference (VTC), Chicago, USA, August 2018 [1].

A. Chawla and A. K. Jagannatham are with the Department of Electrical Engineering, Indian Institute of Technology Kanpur, Kanpur, UP 208016, India (e-mail: {capoorva, adityaj}@iitk.ac.in).

A. Patel and P. K. Varshney are with the Department of Electrical Engineering and Computer Science, Syracuse University, NY 13244, USA (e-mail: {apatel31, varshney}@syr.edu). This work is supported partially by the TCS Research Scholarship Program and DST-SERB Project Grant.

A. Review of Existing Work

Distributed detection over a multiple access channel (MAC) was first investigated in [13]. Berger et al. [14] have examined the performance of decentralized detection for both parallel as well as multiple access channels with noncoherent modulation and censoring, where the FC has a single antenna. In [15], the authors have demonstrated the optimality of the energy detector for a Rayleigh fading scenario for MAC with an infinite number of non-identical sensors in MIMO WSNs. Distributed detection over MIMO channels with a finite number of sensors was initially considered in [16], which presented a power allocation scheme based on the J-divergence criterion in order to optimize the detection performance at the FC. Authors in [17], [18] presented the optimal detection rules and the corresponding performance analysis for cooperative spectrum sensing in multiuser MIMO cognitive radio networks, considering both perfect and imperfect CSI scenarios. Cheng et al. in [19] study the detection performance of a distributed sensor network based on quantized outputs of the local sensor signals. The work in [20] proposed various computationally efficient albeit sub-optimal fusion rules for decision fusion in MIMO WSNs over a coherent MAC. The work in [21] proposed algorithms for the optimal transmission of analog observations, rather than local decisions, in an amplify and forward-based WSN, that maximized the negative exponent of the probability of error at the FC. In [22], the authors determine the optimal decision rules for distributed detection in a scenario wherein the sensors transmit their amplified analog observations to a multi-antenna FC using a fixed transmission gain, followed by analysis to characterize the probabilities of detection and false alarm for different availabilities of channel state information (CSI). The work in [23] considers a distributed WSN, where single-antenna sensors observe an unknown deterministic parameter and simultaneously transmit their phase-shifted and noisy analog observations to the FC over a coherent MAC. The authors in [24] consider a distributed detection system where the sensors transmit their analog observations to the FC with multiple antennas over coherent MAC using the amplify-and forward scheme. The performance of the system is evaluated in terms of the error exponent of the probability of error

and is compared when the channels between the sensors and the FC are AWGN, Rayleigh and Ricean fading, respectively. However, as described in [8], such schemes based on the transmission of analog observations require a large bandwidth and tend to employ classical signal processing schemes that are complex.

Recently, a few works have investigated the impact of employing a massive antenna array at the FC in WSNs. The authors in [25] have studied the estimation and detection performance of a coherent amplify-and-forward WSN with a massive antenna array at the FC, where the performance of the Neyman-Pearson (NP) detector, energy detector, and linear minimum mean squared error (LMMSE) estimator are determined analytically. Decentralized estimation of a correlated random parameter vector in a massive MIMO system over a coherent MAC using the MMSE estimator has been studied in [26]. In [27], the authors have investigated the effects of transceiver hardware impairments, both at the massive-antenna FC and single-antenna sensor nodes, on the detection performance of the FC. In [28], sub-optimal fusion rules with reduced complexity, i.e., linear-filter and deflection-maximizer widely linear (WL) rules, are derived for WSNs where the FC is employed with a large number of antennas. The recent study in [29] derives sub-optimal fusion rules for a Rician fading MAC utilizing only statistical CSI.

In the conference version of this paper [1], we have presented NP criterion based fusion rules where antipodal signaling scheme was utilized for both perfect and imperfect CSI scenarios. Further, closed form expressions were derived to characterize the resulting system probabilities of detection and false alarm at the FC. In this work, the analysis is extended to non-antipodal signaling along with the derivation of closed form expressions of system probabilities of detection and false alarm at the FC. Moreover, signaling matrices are derived considering perfect as well as imperfect CSI for both antipodal and non-antipodal signaling schemes. In addition, asymptotic system performance is analyzed for a large number of antennas at the FC and probability of error expressions are obtained for the preceding scenarios. The main contributions of this work are summarized below.

B. Main Contributions

The main contributions of this paper in the context of distributed detection in a massive MIMO WSN are as follows.

- This work considers a multiple observation vector model in contrast to [28], where binary phase-shift keying (BPSK) modulation was employed to map the decision of each sensor. Here, each sensor transmits decision vectors over one or more signaling intervals corresponding to its local decision, unlike [21], [23], [24] that are based on the transmission of analog observations. Thus, the sensor decisions in this work are prone to error during transmission with a finite probability, in turn making this model more general.
- Low-complexity fusion rules for the low communication channel SNR regime are derived based on linear filtering at the FC while also incorporating the probabilities of detection P_D and false alarm P_{FA} for local sensor decisions, which is absent in [21], [23], [24] that are based entirely on the transmission of analog observations. Antipodal as well as non-antipodal signaling formats are considered for the decision vectors in our analysis. Further, the FC combines the analog signal outputs of the different sensors in contrast to the work in [19] that considers quantized outputs of sensor signals.
- Closed-form analytical expressions are determined to characterize the P_D, P_{FA} performance of the proposed fusion rules at the FC. The above analysis including the decision rules and the corresponding performance is also extended to a scenario with imperfect CSI, whereas [21], [23], [24] consider only perfect CSI.
- The asymptotic system performance is characterized in the large antenna regime, from which it can be inferred that the transmit power of each sensor can be scaled down proportional to the number of antennas at the FC for perfect CSI and similarly, proportional to the square root of the number of antennas for imperfect CSI scenarios.
- Further, the signaling matrices are derived for the WSN to maximize the detection performance at the FC for all the scenarios. It is worth noting that most of the existing works reviewed in Section I-A consider either on-off keying [7], [14], [16], [29] or BPSK modulation [8], [20], [28] while deriving the pertinent detection rules. In contrast, this work presents a comprehensive analysis wherein the fusion rules are derived for both antipodal and non-antipodal signaling schemes, thus making it suitable for a large number of applications.
- Simulation studies are presented to compare the performance of the proposed schemes with the existing techniques and also to validate the theoretical findings.

C. Organization

The outline of the paper is as follows. Section II describes the multiple observation vector based system model for a massive MIMO WSN, where the sensors transmit vectors corresponding to their local decisions over a MAC that are prone to errors with finite probability. Section III derives the likelihood ratio test (LRT)-based detection rules for the scenario with perfect CSI, along with the closed-form expressions for P_D and P_{FA}. The LRT based detection rules incorporating CSI uncertainty are obtained in Section IV. Results characterizing their performance are also presented therein. Section V develops the framework to obtain transmission matrices, followed by the large antenna array analysis in Section VI and detection performance analysis in Section VII. Simulation results are presented in Section VIII, followed by conclusions in Section IX.

D. Notation

For convenience, the notation used throughout the paper is summarized below. Boldface lowercase letters $\mathbf{x}$ are used to denote vectors, where x_n represents the nth component of $\mathbf{x}$ and $\mathbf{x}^{(i)}$ is the vector obtained at the ith iteration. $\mathbf{0}_N$ denotes a $N \times 1$ vector with all its entries being zero. Similarly, boldface uppercase letters $\mathbf{X}$ are employed to denote matrices, where

$[\mathbf{X}]_{m,n}$ represents the (m,n)th component of matrix $\mathbf{X}$ and $\mathbf{X}^{(i)}$ denotes the matrix evaluated at the ith iteration. The matrix $\mathbf{I}_N$ represents an identity matrix of size $N \times N$. The operators $\mathbb{E}\{\cdot\}$, $\Re\{\cdot\}$, $(\cdot)^T$, $(\cdot)^H$, $\exp\{\cdot\}$, $||\cdot||$, vec$(\cdot)$, vec$^{-1}(\cdot)$ and $\otimes$ denote the expectation operator, real part, transpose, conjugate transpose, exponential function, Euclidean norm, vec operator, inverse vec operator and Kronecker product respectively. Pr$(\cdot)$ represents the probability and Pr$(A|B)$ denotes the conditional probability of the event A given B. Similarly, $p(.)$ is used to represent the probability density function (PDF) and $p(A|B)$ denotes the conditional pdf of A given B. The random vector $\mathbf{x} \sim \mathcal{CN}(\boldsymbol{\mu}, \mathbf{R})$ follows a complex Gaussian distribution with mean $\boldsymbol{\mu}$ and covariance matrix $\mathbf{R}$. The quantity Q denotes the Gaussian Q-function, which is defined as $Q(x) = \frac{1}{\sqrt{2\pi}} \int_x^\infty \exp(-\frac{y^2}{2})dy$.

II. SYSTEM MODEL

Consider a distributed detection framework where multiple sensors observe the phenomenon generating a signal of interest, the source of which is assumed to be located at a known location. This scenario can be modeled as a distributed binary hypothesis testing problem, where the null hypothesis $\mathcal{H}_0$ and the alternative hypothesis $\mathcal{H}_1$ denote the absence and presence of the signal of interest, respectively. The WSN comprises of K single-antenna sensors and a FC with a large antenna array of M antennas, such that $M \gg K$, as shown in Fig.1. The sensors communicate with the FC over a flat fading coherent MAC. Depending on the local binary decision, the kth sensor, $1 \leq k \leq K$, transmits the symbols $x_k(1), x_k(2), \ldots, x_k(L)$ over L signaling intervals, which are represented by the vector $\mathbf{x}_k = [x_k(1), x_k(2), \ldots, x_k(L)]^T \in \mathbb{C}^{L\times 1}$. The transmitted local binary decision vectors are either $\mathbf{x}_k = \mathbf{u}_{k,0}$ or $\mathbf{x}_k = \mathbf{u}_{k,1}$, indicating the absence or presence of the signal of interest, respectively. Let the local detection performance of the kth sensor be characterized by its probabilities of detection $(P_{D,k})$ and false alarm $(P_{F,k})$, defined as

$$\begin{aligned} P_{D,k} &= \Pr(\mathbf{x}_k = \mathbf{u}_{k,1}|\mathcal{H}_1), \\ P_{F,k} &= \Pr(\mathbf{x}_k = \mathbf{u}_{k,1}|\mathcal{H}_0). \end{aligned} \tag{1}$$

The signal $\mathbf{y}(l) \in \mathbb{C}^{M\times 1}$ received at the lth, $1 \leq l \leq L$, signaling interval at the FC can be represented as

$$\mathbf{y}(l) = \sqrt{p_u}\mathbf{G}\mathbf{x}(l) + \mathbf{n}(l), \tag{2}$$

where p_u denotes the average transmit power of each sensor and $\mathbf{x}(l) = [x_1(l), \ldots, x_K(l)]^T \in \mathbb{C}^{K\times 1}$ is the vector comprising of the symbols transmitted by the K sensors at the lth signaling interval. The additive noise vector $\mathbf{n}(l) \in \mathbb{C}^{M\times 1}$ is distributed as $\mathbf{n}(l) \sim \mathcal{CN}(\mathbf{0}, \sigma_n^2\mathbf{I}_M)$ and the MIMO channel matrix between the FC and K sensors is represented by $\mathbf{G} \in \mathbb{C}^{M\times K}$. The channel coefficient between the mth, $1 \leq m \leq M$, antenna at the FC and the kth sensor, i.e., $g_{mk} = [\mathbf{G}]_{mk}$, can be characterized as

$$g_{mk} = h_{mk}\sqrt{\beta_k}, \tag{3}$$

where h_{mk} denotes the small-scale fading coefficient between the mth antenna and the kth user that is assumed to be independent and identically distributed (i.i.d.) complex Gaussian with zero mean and unit variance, i.e., $h_{mk} \sim \mathcal{CN}(0,1)$. The large-scale fading coefficient β_k represents the pathloss and log-normal shadowing effects. It is assumed to be fixed over several coherence intervals and is hence invariant across m. Therefore, the resulting channel matrix $\mathbf{G}$ can be modeled as

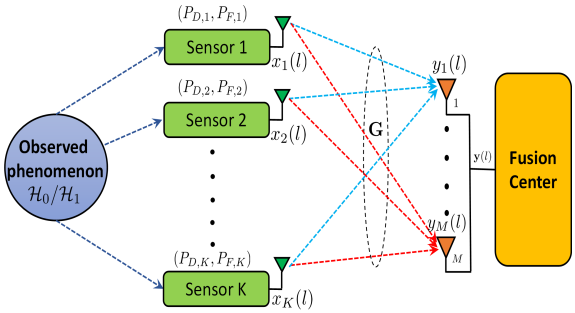

Fig. 1. System model of the massive MIMO wireless sensor network consisting of K single-antenna sensors, communicating with a fusion center equipped with M receive antennas.

$$\mathbf{G} = \mathbf{H}\mathbf{D}^{1/2}, \tag{4}$$

where the diagonal matrix $\mathbf{D} \in \mathbb{C}^{K\times K}$ denotes the matrix with the large-scale fading coefficients β_k, $1 \leq k \leq K$, along its principal diagonal, i.e., $[\mathbf{D}]_{kk} = \beta_k$. The small-scale fading coefficient matrix $\mathbf{H} \in \mathbb{C}^{M\times K}$, with its elements $[\mathbf{H}]_{mk} = h_{mk}$, is defined above in (3). Therefore, the received signal matrix $\mathbf{Y} = [\mathbf{y}(1), \ldots, \mathbf{y}(l), \ldots, \mathbf{y}(L)] \in \mathbb{C}^{M\times L}$ at the FC for the L received signal vectors $\mathbf{y}(l)$, described in (2), can be represented as

$$\mathbf{Y} = \sqrt{p_u}\mathbf{G}\mathbf{X} + \mathbf{N}, \tag{5}$$

where $\mathbf{X} = [\mathbf{x}(1), \ldots, \mathbf{x}(L)] \in \mathbb{C}^{K\times L}$ is the concatenated transmitted signal matrix corresponding to the L composite signal vectors $\mathbf{x}(l), 1 \leq l \leq L$, and the noise matrix $\mathbf{N} \in \mathbb{C}^{M\times L}$ is obtained by stacking the L circularly symmetric AWGN vectors $\mathbf{n}(l), 1 \leq l \leq L$, such that its elements are distributed as $n_{i,j}(l) \sim \mathcal{CN}(0, \sigma_n^2)$. The elements of the channel matrix $\mathbf{G}$ are assumed to be modeled as independent random variables which follow the complex Gaussian distribution, i.e., $g_{mk} \sim \mathcal{CN}(0, \beta_k)$, under favorable propagation conditions [5], [30]. This follows from the assumption that the sensors in the massive MIMO WSN are spatially separated by large distances. Moreover, different column vectors of the channel matrix $\mathbf{G}$ associated with the different sensors are assumed to be mutually independent. Therefore, using the law of large numbers it follows that

$$\frac{1}{M}\mathbf{G}^H\mathbf{G} \approx \mathbf{D}, \quad \text{for } M \gg K. \tag{6}$$

Hence, the channel vectors corresponding to the different sensors are asymptotically pairwise orthogonal for the scenario with a large antenna array employed at the FC coupled with favorable propagation conditions. Using the above framework for massive MIMO WSN, the subsequent sections present the fusion rules for various scenarios.

III. FUSION RULE WITH PERFECT CSI

In this section, fusion rules are derived for a scenario with perfect CSI considering for both antipodal and non

antipodal signaling schemes. Employing the Neyman-Pearson (NP) criterion that aims to maximize the detection probability for a given probability of false alarm, the log likelihood ratio (LLR) $T(\mathbf{Y})$ for the observation matrix $\mathbf{Y}$ defined in (5), and the corresponding test are given as

$$T(\mathbf{Y}) = \ln\left[\frac{p(\mathbf{Y}|\mathcal{H}_1)}{p(\mathbf{Y}|\mathcal{H}_0)}\right] \underset{\mathcal{H}_0}{\overset{\mathcal{H}_1}{\gtrless}} \gamma, \tag{7}$$

where γ denotes the decision threshold. The quantities $p(\mathbf{Y}|\mathcal{H}_1)$ and $p(\mathbf{Y}|\mathcal{H}_0)$ in the above expression (7) represent the probability density functions (PDFs) of the received matrix $\mathbf{Y}$ under the alternative and null hypotheses, respectively. Utilizing the independence of the transmitted signal vectors, i.e., $\mathbf{x}(l)$ across the L different signaling intervals, the simplified expression for the LLR test in (7) can be expressed as

$$T(\mathbf{Y}) = \sum_{l=1}^{L} \ln\left[\frac{\sum_{\mathbf{x}(l)} p\left(\mathbf{y}(l)|\mathbf{x}(l)\right) \Pr\left(\mathbf{x}(l)|\mathcal{H}_1\right)}{\sum_{\mathbf{x}(l)} p\left(\mathbf{y}(l)|\mathbf{x}(l)\right) \Pr\left(\mathbf{x}(l)|\mathcal{H}_0\right)}\right] \tag{8}$$

$$= \sum_{l=1}^{L} \ln\left[\frac{\sum\limits_{\mathbf{x}(l)} \exp\left(-\frac{\|\mathbf{y}(l)-\sqrt{p_u}\mathbf{G}\mathbf{x}(l)\|^2}{\sigma_n^2}\right)\Pr(\mathbf{x}(l)|\mathcal{H}_1)}{\sum\limits_{\mathbf{x}(l)} \exp\left(-\frac{\|\mathbf{y}(l)-\sqrt{p_u}\mathbf{G}\mathbf{x}(l)\|^2}{\sigma_n^2}\right)\Pr(\mathbf{x}(l)|\mathcal{H}_0)}\right], \tag{9}$$

where the PDF of $\mathbf{y}(l)$ for a given $\mathbf{x}(l)$, i.e., $p\left(\mathbf{y}(l)|\mathbf{x}(l)\right)$, follows the Gaussian distribution, given as

$$p(\mathbf{y}(l)|\mathbf{x}(l)) = \frac{1}{(\pi\sigma_n^2)^M} \exp\left[\frac{-1}{\sigma_n^2}\|\mathbf{y}(l)-\sqrt{p_u}\mathbf{G}\mathbf{x}(l)\|^2\right]. \tag{10}$$

However, it can be observed that the LLR test in (9) is computationally complex and numerically unstable. This is due to the summation over 2^K exponential terms with a large dynamic range in the numerator as well as in the denominator [20], [28]. Therefore, to present $T(\mathbf{Y})$ in a more stable form which is amenable to numerical implementation, it can be approximated by a two step procedure. In the first step, the received signal is processed with the help of linear matched filtering to obtain the outputs corresponding to the individual sensors. Subsequently, the second step derives a final decision by combining the individual sensor decisions. A similar two step approach is used in [28] that presents different linear processing techniques, namely the matched filter (MF), zero forcing (ZF) and minimum mean squared error (MMSE) techniques, to characterize the performance of the massive MIMO WSN. However, the work in this paper focuses on a comprehensive analysis that includes obtaining the probabilities of detection, false alarm and error, the corresponding power scaling laws, and also the structure of the transmission matrices, which are lacking in [28]. The analysis for ZF is similar and is shown in Appendix A.

The output matrix $\mathbf{Z} = [\mathbf{z}(1), \ldots, \mathbf{z}(L)] \in \mathbb{C}^{K\times L}$ obtained after matched filtering the received matrix $\mathbf{Y}$ in (5) is

$$\mathbf{Z} = \mathbf{G}^H\mathbf{Y} = \sqrt{p_u}\mathbf{G}^H\mathbf{G}\mathbf{X} + \tilde{\mathbf{N}}, \tag{11}$$

where $\tilde{\mathbf{N}} = \mathbf{G}^H\mathbf{N} \in \mathbb{C}^{K\times L}$ denotes the equivalent noise matrix after filtering. From (11), it can be noticed that for a given vector $\mathbf{x}(l)$, the lth column $\mathbf{z}(l)$ of the filter matrix $\mathbf{Z}$ follows the complex Normal distribution described as $\mathcal{CN}(\sqrt{p_u}\mathbf{G}^H\mathbf{G}\mathbf{x}(l), \sigma_n^2\mathbf{G}^H\mathbf{G})$. Under the favorable propagation conditions stated in (6), the equivalent system model for the lth filter output vector $\mathbf{z}(l) = [z_1(l), \ldots, z_K(l)]^T \in \mathbb{C}^{K\times 1}$ can be expressed as

$$\mathbf{z}(l) = \sqrt{p_u}M\mathbf{D}\mathbf{x}(l) + \tilde{\mathbf{n}}(l), \tag{12}$$

where $\tilde{\mathbf{n}}(l) \in \mathbb{C}^{K\times 1}$ distributed as $\mathcal{CN}(\mathbf{0}, M\mathbf{D}\sigma_n^2)$ represents the lth column vector of the noise matrix $\tilde{\mathbf{N}}$. Similarly, from (11) and (12), the filter output vector $\mathbf{z}_k = [z_k(1), \ldots, z_k(L)]^T \in \mathbb{C}^{L\times 1}$ corresponding to the kth user over L signaling intervals can be equivalently written as

$$\mathbf{z}_k = \sqrt{p_u}M\beta_k\mathbf{x}_k + \tilde{\mathbf{n}}_k. \tag{13}$$

The lth component $z_k(l)$ of the filter output vector $\mathbf{z}_k$ can now be modeled as $z_k(l) \sim \mathcal{CN}(\sqrt{p_u}M\beta_k x_k(l), M\beta_k\sigma_n^2)$. Hence, it can be equivalently represented as a parallel access channel (PAC) between the sensors and the FC, as a consequence of the linear processing and the large antenna array employed at the FC. Thus, exploiting the independence of the signal vectors across the K sensors, the LLR test for distributed detection in the massive MIMO WSN described in (13) under ideal CSI can be formulated as

$$T(\mathbf{Z}) = \ln\left[\frac{p(\mathbf{Z}|\mathcal{H}_1)}{p(\mathbf{Z}|\mathcal{H}_0)}\right] = \ln\left[\prod_{k=1}^{K}\frac{p(\mathbf{z}_k|\mathcal{H}_1)}{p(\mathbf{z}_k|\mathcal{H}_0)}\right], \tag{14}$$

where $p(\mathbf{z}_k|\mathcal{H}_0)$ and $p(\mathbf{z}_k|\mathcal{H}_1)$ denote the PDFs of the received vector $\mathbf{z}_k$ under the null and alternative hypotheses, respectively. For $\mathbf{u}_k \in \{\mathbf{u}_{k,0}, \mathbf{u}_{k,1}\}$, the above LLR test can be expressed as shown in (15).

The authors in [18] show that different signaling schemes with the same transmit power have different detection performances. Therefore, the performance of the proposed rules is presented for antipodal as well as non-antipodal signaling schemes. The subsequent subsections individually simplify and analyze the performance of the test in (15) for both signaling formats.

A. Antipodal Signaling

Consider the transmit signal vectors $\mathbf{u}_{k,0} = -\mathbf{u}_k$ and $\mathbf{u}_{k,1} = \mathbf{u}_k$ for the kth user, corresponding to the absence and presence of the signal of interest, respectively. The PDFs of the observation vector $\mathbf{z}_k$ for the antipodal signaling vectors $-\mathbf{u}_k, \mathbf{u}_k$ are given as

$$p(\mathbf{z}_k|\mathbf{x}_k{=}-\mathbf{u}_k){=}\frac{1}{(\pi M\beta_k\sigma_n^2)^L}\exp\left(\frac{-\|\mathbf{z}_k+\sqrt{p_u}M\beta_k\mathbf{u}_k\|^2}{M\beta_k\sigma_n^2}\right), \tag{17}$$

$$p(\mathbf{z}_k|\mathbf{x}_k = \mathbf{u}_k){=}\frac{1}{(\pi M\beta_k\sigma_n^2)^L}\exp\left(\frac{-\|\mathbf{z}_k-\sqrt{p_u}M\beta_k\mathbf{u}_k\|^2}{M\beta_k\sigma_n^2}\right). \tag{18}$$

Substituting the above PDFs in (15), the test statistic for this case can be derived as shown in (16), which can be further simplified to the expression below

$$T_{\mathrm{A}}(\mathbf{Z}){=}\sum_{k=1}^{K}\ln\left[\frac{P_{D,k}+(1{-}P_{D,k})\exp\left(\frac{-4\sqrt{p_u}}{\sigma_n^2}\Re(\mathbf{z}_k^H\mathbf{u}_k)\right)}{P_{F,k}+(1-P_{F,k})\exp\left(\frac{-4\sqrt{p_u}}{\sigma_n^2}\Re(\mathbf{z}_k^H\mathbf{u}_k)\right)}\right], \tag{19}$$

$$T(\mathbf{Z}) = \ln\Big[\prod_{k=1}^{K}\frac{p(\mathbf{z}_k|\mathcal{H}_1)}{p(\mathbf{z}_k|\mathcal{H}_0)}\Big] = \sum_{k=1}^{K}\ln\Big[\frac{p(\mathbf{z}_k|\mathbf{x}_k=\mathbf{u}_{k,1})\Pr(\mathbf{x}_k=\mathbf{u}_{k,1}|\mathcal{H}_1)+p(\mathbf{z}_k|\mathbf{x}_k=\mathbf{u}_{k,0})\Pr(\mathbf{x}_k=\mathbf{u}_{k,0}|\mathcal{H}_1)}{p(\mathbf{z}_k|\mathbf{x}_k=\mathbf{u}_{k,1})\Pr(\mathbf{x}_k=\mathbf{u}_{k,1}|\mathcal{H}_0)+p(\mathbf{z}_k|\mathbf{x}_k=\mathbf{u}_{k,0})\Pr(\mathbf{x}_k=\mathbf{u}_{k,0}|\mathcal{H}_0)}\Big] \tag{15}$$

$$T_{\mathrm{A}}(\mathbf{Z}) = \sum_{k=1}^{K}\ln\left[\frac{P_{D,k}\exp\Big(-\frac{\|\mathbf{z}_k-\sqrt{p_u}M\beta_k\mathbf{u}_k\|^2}{M\beta_k\sigma_n^2}\Big)+(1-P_{D,k})\exp\Big(-\frac{\|\mathbf{z}_k+\sqrt{p_u}M\beta_k\mathbf{u}_k\|^2}{M\beta_k\sigma_n^2}\Big)}{P_{F,k}\exp\Big(-\frac{\|\mathbf{z}_k-\sqrt{p_u}M\beta_k\mathbf{u}_k\|^2}{M\beta_k\sigma_n^2}\Big)+(1-P_{F,k})\exp\Big(-\frac{\|\mathbf{z}_k+\sqrt{p_u}M\beta_k\mathbf{u}_k\|^2}{M\beta_k\sigma_n^2}\Big)}\right] \tag{16}$$

In order to analyze the performance of the detector, the above test statistic can be further simplified for the low SNR regime as described next [18]. Using the approximations $e^{-v}\approx(1-v)$ and $\ln(1+v)\approx v$ that hold for sufficiently small values of v, the test statistic in (19) can be simplified as

$$T_{\mathrm{A}}(\mathbf{Z}) = \sum_{k=1}^{K} a_k\Re(\mathbf{z}_k^H\mathbf{u}_k)\underset{\mathcal{H}_0}{\overset{\mathcal{H}_1}{\gtrless}}\gamma_{\mathrm{AP}}, \tag{20}$$

where $a_k \triangleq P_{D,k}-P_{F,k}$ denotes the constant corresponding to the kth sensor. It is worth noting that the low SNR assumption is related to the SNR of the communication channel, i.e., $p_u \ll \sigma_n^2$. The above test considers a general case with imperfect sensors, i.e., $P_{D,k}\neq 1$ and $P_{F,k}\neq 0$ in contrast to the one in [28], which considers an ideal scenario with perfect sensors for the MRC and MMRC fusion rules. Further, the simplified test statistic obtained above has a lower computational complexity due to its linear structure in comparison to some of the tests in [28] such as the decode-then-fuse approach based rules. Also, the analysis above considers a general scenario with transmission of multiple symbols over L signaling intervals. The low SNR approximation based test statistic is applicable to practical scenarios as WSNs are typically resource constrained in terms of the transmit power [12], [31]. Furthermore, it is often desirable to limit the transmit signal power of the sensors in order to minimize the probability of unauthorized interception/ detection [10]. The result below describes the performance of the test in terms of the resulting P_D and P_{FA}. It is worth noting that such analytical results have not been given in the existing works such as [21], [23], [24].

Theorem 1. *The probabilities of detection (P_D) and false alarm (P_{FA}) corresponding to the test statistic in* (20) *for distributed detection at the FC with perfect CSI under antipodal signaling are*

$$P_D = Q\left(\frac{\gamma_{AP}-\mu_{T_A|\mathcal{H}_1}}{\sigma_{T_A|\mathcal{H}_1}}\right), \tag{21}$$

$$P_{FA} = Q\left(\frac{\gamma_{AP}-\mu_{T_A|\mathcal{H}_0}}{\sigma_{T_A|\mathcal{H}_0}}\right), \tag{22}$$

where the quantities $\mu_{T_A|\mathcal{H}_0}, \mu_{T_A|\mathcal{H}_1}$ and $\sigma^2_{T_A|\mathcal{H}_0}, \sigma^2_{T_A|\mathcal{H}_1}$ represent the means and variances of the test statistic $T_A(\mathbf{Z})$ under the null and alternative hypotheses, respectively, which are obtained as

$$\mu_{T_A|\mathcal{H}_0} = \sum_{k=1}^{K}\sqrt{p_u}a_k c_k M\beta_k\|\mathbf{u}_k\|^2, \tag{23}$$

$$\mu_{T_A|\mathcal{H}_1} = \sum_{k=1}^{K}\sqrt{p_u}a_k b_k M\beta_k\|\mathbf{u}_k\|^2, \tag{24}$$

$$\sigma^2_{T_A|\mathcal{H}_0} = \sum_{k=1}^{K} M\beta_k a_k^2\|\mathbf{u}_k\|^2\Big(p_u M\beta_k(1-c_k^2)\|\mathbf{u}_k\|^2+\frac{\sigma_n^2}{2}\Big), \tag{25}$$

$$\sigma^2_{T_A|\mathcal{H}_1} = \sum_{k=1}^{K} M\beta_k a_k^2\|\mathbf{u}_k\|^2\Big(p_u M\beta_k(1-b_k^2)\|\mathbf{u}_k\|^2+\frac{\sigma_n^2}{2}\Big), \tag{26}$$

where the constants a_k and b_k for the kth user are defined as $b_k = 2P_{D,k}-1$ and $c_k = 2P_{F,k}-1$ and γ_{AP} denotes the detection threshold in (20)*.*

Proof: See Appendix A in [1]. ■

B. Non-Antipodal Signaling

Consider now the non-antipodal signaling scenario, i.e., $\mathbf{u}_{k,0}=\mathbf{0}$ and $\mathbf{u}_{k,1}=\mathbf{u}_k$ indicating the kth user's decision corresponding to the null and alternative hypotheses, respectively. Therefore, the conditional PDFs of $\mathbf{z}_k$ in (13) with the non-antipodal signaling constellation above is expressed as

$$p(\mathbf{z}_k|\mathbf{x}_k=\mathbf{0}) \sim \mathcal{CN}(\mathbf{0}, M\beta_k\sigma_n^2\mathbf{I}), \tag{27}$$

$$p(\mathbf{z}_k|\mathbf{x}_k=\mathbf{u}_k) \sim \mathcal{CN}(\sqrt{p_u}M\beta_k\mathbf{u}_k, M\beta_k\sigma_n^2\mathbf{I}). \tag{28}$$

Using the substitution $\mathbf{z}'_k = \mathbf{z}_k - \sqrt{p_u}M\beta_k\frac{\mathbf{u}_k}{2}$ and defining $\mathbf{Z}' = [\mathbf{z}'(1),\ldots,\mathbf{z}'(L)] \in \mathbb{C}^{K\times L}$, the conditional PDFs of $\mathbf{z}'_k$ corresponding to $\mathbf{x}_k = \{\mathbf{0},\mathbf{u}_k\}$ follow as

$$p(\mathbf{z}'_k|\mathbf{x}_k=\mathbf{0}) \sim \mathcal{CN}(-\sqrt{p_u}M\beta_k\mathbf{u}_k/2, M\beta_k\sigma_n^2\mathbf{I}), \tag{29}$$

$$p(\mathbf{z}'_k|\mathbf{x}_k=\mathbf{u}_k) \sim \mathcal{CN}(\sqrt{p_u}M\beta_k\mathbf{u}_k/2, M\beta_k\sigma_n^2\mathbf{I}), \tag{30}$$

which are similar to (17), (18). Hence, the test $T_{\mathrm{N}}(\mathbf{Z}')$ under non-antipodal signaling can be determined similar to (19) as

$$T_{\mathrm{N}}(\mathbf{Z}') = \sum_{k=1}^{K}\ln\left[\frac{P_{D,k}+(1-P_{D,k})\exp\big(\frac{-2\sqrt{p_u}}{\sigma_n^2}\Re(\mathbf{z}_k'^H\mathbf{u}_k)\big)}{P_{F,k}+(1-P_{F,k})\exp\big(\frac{-2\sqrt{p_u}}{\sigma_n^2}\Re(\mathbf{z}_k'^H\mathbf{u}_k)\big)}\right]. \tag{31}$$

Following the procedure used in (20), the above test statistic can be simplified to yield the closed-form expression below

$$T_{\mathrm{N}}(\mathbf{Z}') = \sum_{k=1}^{K} a_k\Re(\mathbf{z}_k'^H\mathbf{u}_k)\underset{\mathcal{H}_0}{\overset{\mathcal{H}_1}{\gtrless}}\gamma_{\mathrm{NP}}, \tag{32}$$

where $a_k \triangleq P_{D,k}-P_{F,k}$ and γ_{NP} is the detection threshold. The pertinent detectors and the analysis for the non-antipodal signaling format considered above have not been given in [28].

Note : The probabilities of detection (P_D) and false alarm (P_{FA}) for the above mentioned test under non-antipodal signaling can be obtained by replacing the quantity p_u in (23), (24), (25) and (26) by $\frac{p_u}{4}$.

The analysis in this section considered perfect CSI to be available at the FC. However, in practical scenarios, the CSI at the FC is obtained via channel estimation, which leads to errors in the estimated CSI. The next section determines the

fusion rules and also presents the pertinent analysis considering CSI uncertainty in massive MIMO WSNs.

IV. Fusion Rules under CSI Uncertainty

For scenarios with CSI uncertainty, the true channel matrix $\mathbf{G}$ can be characterized as

$$\mathbf{G} \triangleq \hat{\mathbf{G}} - \mathcal{E}, \tag{33}$$

where $\hat{\mathbf{G}} \in \mathbb{C}^{M\times K}$ represents the estimate of the channel matrix and the matrix $\mathcal{E} = [\mathbf{e}_1, \ldots, \mathbf{e}_K] \in \mathbb{C}^{M\times K}$ denotes the error matrix pertaining to the channel estimate similar to [32], [33]. Similar to [6], consider the transmission of the orthogonal pilot matrix $\mathbf{\Phi} \in \mathbb{C}^{\tau_p\times K}$, i.e., $\mathbf{\Phi}^H\mathbf{\Phi} = \mathbf{I}_K$, for the purpose of channel estimation. It is assumed that τ_p symbols are used as pilots and τ_d symbols are used for transmitting data, such that $\tau_p + \tau_d \leq \tau_c$, where τ_c denotes the coherence interval. The system model for channel estimation from the transmitted pilots is

$$\mathbf{Y}_p = \sqrt{p_p}\mathbf{G}\mathbf{\Phi}^T + \mathbf{N}_p, \tag{34}$$

where p_p denotes the pilot power, i.e. $p_p \triangleq \tau_p p_u$. Therefore, the MMSE estimate of $\mathbf{G}$ is

$$\hat{\mathbf{G}} = \frac{1}{\sqrt{p_p}}\mathbf{Y}_p\mathbf{\Phi}^*\left(\frac{\sigma_n^2}{p_p}\mathbf{D}^{-1} + \mathbf{I}_K\right)^{-1}. \tag{35}$$

As shown in [6], the resulting estimate $\hat{\mathbf{g}}_k$ and the corresponding error $\mathbf{e}_k$ are distributed as

$$\hat{\mathbf{g}}_k \sim \mathcal{CN}(\mathbf{0}, \tilde{\beta}_k\mathbf{I}_M), \text{where } \tilde{\beta}_k \triangleq p_p\beta_k^2/(\sigma_n^2 + p_p\beta_k), \tag{36}$$

$$\mathbf{e}_k \sim \mathcal{CN}(\mathbf{0}, \gamma_{e,k}\mathbf{I}_M), \text{where } \gamma_{e,k} \triangleq \sigma_n^2\beta_k/(\sigma_n^2 + p_p\beta_k). \tag{37}$$

Therefore, the equivalent system model for (5), incorporating the CSI uncertainty, can be obtained as

$$\mathbf{Y} = \sqrt{p_u}(\hat{\mathbf{G}} - \mathcal{E})\mathbf{X} + \mathbf{N} = \sqrt{p_u}\hat{\mathbf{G}}\mathbf{X} + \mathbf{W}, \tag{38}$$

where $\mathbf{W} \in \mathbb{C}^{M\times L}$ denotes the equivalent noise matrix defined as, $\mathbf{W} \triangleq \mathbf{N} - \sqrt{p_u}\mathcal{E}\mathbf{X}$. It follows from the distributions of column vectors in $\mathbf{N}$, $\mathcal{E}$, given in (36), (37), respectively, that the lth column vector of the noise matrix $\mathbf{W}$, i.e., $\mathbf{w}(l)$ follows the complex Gaussian distribution with zero mean and covariance matrix $\mathbf{R}_{w(l)} = \mathbb{E}\{\mathbf{w}(l)\mathbf{w}^H(l)\} = \sigma_w^2\mathbf{I}_M$ with $\sigma_w^2 = p_u\sum_{k=1}^K |u_{k,i}(l)|^2\gamma_{e,k} + \sigma_n^2$. Similar to (13), on matched filtering with the estimated channel matrix and exploiting $\frac{1}{M}\hat{\mathbf{G}}^H\hat{\mathbf{G}} \approx \tilde{\mathbf{D}}$ under favorable propagation conditions, where $\tilde{\mathbf{D}}$ is a diagonal matrix with $[\tilde{\mathbf{D}}]_{kk} = \tilde{\beta}_k$, the equivalent system model for the filter output vector $\tilde{\mathbf{z}}_k \in \mathbb{C}^{L\times 1}$ corresponding to the kth user is

$$\tilde{\mathbf{z}}_k = \sqrt{p_u}M\tilde{\beta}_k\mathbf{x}_k + \tilde{\mathbf{w}}_k. \tag{39}$$

Hence, the NP-based test statistic for distributed detection with CSI uncertainty in the massive MIMO WSN is derived as

$$T_{\mathrm{R}}(\tilde{\mathbf{Z}}) = \ln\left[\frac{p(\tilde{\mathbf{Z}}|\mathcal{H}_1)}{p(\tilde{\mathbf{Z}}|\mathcal{H}_0)}\right] \tag{40}$$

Considering the binary transmit vector constellation $\{\mathbf{u}_{k,0}, \mathbf{u}_{k,1}\}$ for the transmit vector $\mathbf{x}_k$, the test above reduces to the one shown in (41). The fusion rules corresponding to antipodal and non-antipodal signaling scenarios are provided below.

A. Fusion rules for Antipodal/ Non-Antipodal Signaling

For the antipodal signaling vectors $\mathbf{x}_{k,0} = -\mathbf{u}_k$ and $\mathbf{x}_{k,1} = \mathbf{u}_k$ corresponding to the null and alternative hypotheses, respectively, the resulting PDFs for $\tilde{\mathbf{z}}_k$ are determined as

$$p(\tilde{\mathbf{z}}_k|\mathbf{x}_k = -\mathbf{u}_k) \sim \mathcal{CN}(-\sqrt{p_u}M\tilde{\beta}_k\mathbf{u}_k, M\tilde{\beta}_k\sigma_w^2\mathbf{I}_L), \tag{42}$$

$$p(\tilde{\mathbf{z}}_k|\mathbf{x}_k = \mathbf{u}_k) \sim \mathcal{CN}(\sqrt{p_u}M\tilde{\beta}_k\mathbf{u}_k, M\tilde{\beta}_k\sigma_w^2\mathbf{I}_L). \tag{43}$$

On substitution of the PDFs above, the test obtained in (41) simplifies to

$$T_{\mathrm{R,A}}(\tilde{\mathbf{Z}}) = \sum_{k=1}^K \ln\left[\frac{P_{D,k} + (1-P_{D,k})\exp\left(\frac{-4\sqrt{p_u}}{\sigma_w^2}\Re(\tilde{\mathbf{z}}_k^H\mathbf{u}_k)\right)}{P_{F,k} + (1-P_{F,k})\exp\left(\frac{-4\sqrt{p_u}}{\sigma_w^2}\Re(\tilde{\mathbf{z}}_k^H\mathbf{u}_k)\right)}\right],$$

which further reduces to the computationally efficient form shown below in the low SNR regime

$$T_{\mathrm{R,A}}(\tilde{\mathbf{Z}}) = \sum_{k=1}^K a_k\Re(\tilde{\mathbf{z}}_k^H\mathbf{u}_k) \underset{\mathcal{H}_0}{\overset{\mathcal{H}_1}{\gtrless}} \gamma_{\mathrm{AI}}. \tag{44}$$

For the specific scenario with $P_{D,k} = P_d$ and $P_{F,k} = P_f, \forall k$, i.e., all the constituent sensors in the WSN have identical local sensing performance, the test statistic further reduces to

$$T_{\mathrm{R,A,I}}(\tilde{\mathbf{Z}}) = \sum_{k=1}^K \Re(\tilde{\mathbf{z}}_k^H\mathbf{u}_k). \tag{45}$$

Theorem 2. *The detection performance of the test in* (44) *for a massive MIMO WSN with CSI uncertainty can be characterized in terms of the resulting P_D, P_{FA} as*

$$P_D = Q\left(\frac{\gamma_{AI} - \mu_{T_{R,A}|\mathcal{H}_1}}{\sigma_{T_{R,A}|\mathcal{H}_1}}\right),\ P_{FA} = Q\left(\frac{\gamma_{AI} - \mu_{T_{R,A}|\mathcal{H}_0}}{\sigma_{T_{R,A}|\mathcal{H}_0}}\right), \tag{46}$$

where γ_{AI} is the detection threshold in (44)*. The quantities $\mu_{T_{R,A}|\mathcal{H}_0}$, $\mu_{T_{R,A}|\mathcal{H}_1}$ and $\sigma^2_{T_{R,A}|\mathcal{H}_0}$, $\sigma^2_{T_{R,A}|\mathcal{H}_1}$ are given similar to the expressions in* (23)*,* (24)*,* (25)*,* (26)*, respectively, with β_k, σ_n^2 replaced by $\tilde{\beta}_k$, σ_w^2, respectively and are given as*

$$\mu_{T_{R,A}|\mathcal{H}_0} = \sum_{k=1}^K \sqrt{p_u}a_k c_k M\tilde{\beta}_k\|\mathbf{u}_k\|^2, \tag{47}$$

$$\mu_{T_{R,A}|\mathcal{H}_1} = \sum_{k=1}^K \sqrt{p_u}a_k b_k M\tilde{\beta}_k\|\mathbf{u}_k\|^2, \tag{48}$$

$$\sigma^2_{T_{R,A}|\mathcal{H}_0} = \sum_{k=1}^K M\tilde{\beta}_k a_k^2\|\mathbf{u}_k\|^2\Big(p_u M\tilde{\beta}_k(1-c_k^2)\|\mathbf{u}_k\|^2 + \frac{\sigma_w^2}{2}\Big), \tag{49}$$

$$\sigma^2_{T_{R,A}|\mathcal{H}_1} = \sum_{k=1}^K M\tilde{\beta}_k a_k^2\|\mathbf{u}_k\|^2\Big(p_u M\tilde{\beta}_k(1-b_k^2)\|\mathbf{u}_k\|^2 + \frac{\sigma_w^2}{2}\Big), \tag{50}$$

with $b_k = 2P_{D,k} - 1$ and $c_k = 2P_{F,k} - 1$.

Proof: See Appendix B. ∎

Once again the same differences apply with respect to the work in [28] as mentioned in Section III-A and Section III-B for scenarios with perfect CSI for the antipodal and non-antipodal signaling schemes. Moreover, the analysis in terms of P_D and P_{FA} is not presented in the existing works such as [21], [23], [24]. Similar to Section III-B, for non-antipodal signaling using the constellation $\{\mathbf{0}, \mathbf{u}_k\}$, one can employ the substitution $\tilde{\mathbf{z}}_k' = \tilde{\mathbf{z}}_k - \sqrt{p_u}M\beta_k\frac{\mathbf{u}_k}{2}$. The output after the

$$T_{\mathrm{R}}(\tilde{\mathbf{Z}}) = \ln\Bigg[\prod_{k=1}^{K}\frac{p(\tilde{\mathbf{z}}_k|\mathcal{H}_1)}{p(\tilde{\mathbf{z}}_k|\mathcal{H}_0)}\Bigg] = \sum_{k=1}^{K}\ln\Bigg[\frac{p(\tilde{\mathbf{z}}_k|\mathbf{x}_k=\mathbf{u}_{k,1})\mathrm{Pr}(\mathbf{x}_k=\mathbf{u}_{k,1}|\mathcal{H}_1)+p(\tilde{\mathbf{z}}_k|\mathbf{x}_k=\mathbf{u}_{k,0})\mathrm{Pr}(\mathbf{x}_k=\mathbf{u}_{k,0}|\mathcal{H}_1)}{p(\tilde{\mathbf{z}}_k|\mathbf{x}_k=\mathbf{u}_{k,1})\mathrm{Pr}(\mathbf{x}_k=\mathbf{u}_{k,1}|\mathcal{H}_0)+p(\tilde{\mathbf{z}}_k|\mathbf{x}_k=\mathbf{u}_{k,0})\mathrm{Pr}(\mathbf{x}_k=\mathbf{u}_{k,0}|\mathcal{H}_0)}\Bigg]. \quad (41)$$

above substitution, for this scenario with CSI uncertainty is now obtained as

$$\tilde{\mathbf{z}}'_k = \sqrt{p_u}M\tilde{\beta}_k\Big(\mathbf{x}_k - \frac{\mathbf{u}_k}{2}\Big) + \tilde{\mathbf{w}}_k, \quad (51)$$

with the corresponding PDFs for $\tilde{\mathbf{z}}'_k$ under the null and alternative hypotheses obtained as

$$p(\tilde{\mathbf{z}}'_k|\mathbf{x}_k=\mathbf{0}) \sim \mathcal{CN}(-\sqrt{p_u}M\tilde{\beta}_k\mathbf{u}_k/2, M\tilde{\beta}_k\sigma_w^2\mathbf{I}), \quad (52)$$

$$p(\tilde{\mathbf{z}}'_k|\mathbf{x}_k=\mathbf{u}_k) \sim \mathcal{CN}(\sqrt{p_u}M\tilde{\beta}_k\mathbf{u}_k/2, M\tilde{\beta}_k\sigma_w^2\mathbf{I}). \quad (53)$$

Substituting the PDFs above in (41) and simplifying, the test statistic for the non-antipodal signaling scenario is given as

$$T_{\mathrm{R,N}}(\tilde{\mathbf{Z}}') = \sum_{k=1}^{K} a_k\Re(\tilde{\mathbf{z}}_k'^H\mathbf{u}_k) \underset{\mathcal{H}_0}{\overset{\mathcal{H}_1}{\gtrless}} \gamma_{\mathrm{NI}}, \quad (54)$$

where $a_k \triangleq P_{D,k} - P_{F,k}$ and γ_{NI} represents the detection threshold, which further reduces to $T_{\mathrm{R,N,I}}(\tilde{\mathbf{Z}}') = \sum_{k=1}^{K}\Re(\tilde{\mathbf{z}}_k'^H\mathbf{u}_k)$ under identical local sensor performance. The P_D, P_{FA} performance can be obtained similar to Theorem 2 by replacing p_u by $\frac{p_u}{4}$ in (47), (48), (49) and (50), respectively.

V. Signaling Matrices

This section presents the optimization framework to determine the transmit signal matrices $\mathbf{X} = [\mathbf{x}_1, \mathbf{x}_2, \ldots, \mathbf{x}_K]^T \in \mathbb{C}^{K\times L}$, where $\mathbf{x}_k \in \{\mathbf{u}_{k,0}, \mathbf{u}_{k,1}\}$, to further improve the performance of the proposed detectors for a massive MIMO WSN. This design problem that can lead to a performance improvement has not been considered in existing works such as [10], [11], [28]. Let the concatenated vector $\mathbf{u} \in \mathbb{C}^{KL\times 1}$, corresponding to the transmit vectors $\mathbf{u}_1, \mathbf{u}_2, \ldots, \mathbf{u}_K$, be defined as $\mathbf{u} = \mathrm{vec}(\mathbf{U}^T) = [\mathbf{u}_1^T, \mathbf{u}_2^T, \ldots, \mathbf{u}_K^T]^T$. One can now maximize the deflection coefficient $d^2(\mathbf{u})$ [34], which determines the detection performance under Gaussian noise,

$$d^2(\mathbf{u}) \triangleq \frac{\big(\mathbb{E}\{T(\mathbf{Z});\mathcal{H}_1\} - \mathbb{E}\{T(\mathbf{Z});\mathcal{H}_0\}\big)^2}{\mathrm{var}\{T(\mathbf{Z});\mathcal{H}_0\}}, \quad (55)$$

where $\mathbb{E}\{T(\mathbf{Z});\mathcal{H}_1\}$, $\mathbb{E}\{T(\mathbf{Z});\mathcal{H}_0\}$ denote the respective means under the two hypotheses and $\mathrm{var}\{T(\mathbf{Z});\mathcal{H}_0\}$ represents the variance of the test statistic $T(\mathbf{Z})$ corresponding to the null hypothesis. It can be further noted that this approach is valid in the low SNR communication regime for which the resulting simplied linear test statistics in (20), (32), (44) and (54) are Gaussian distributed. The procedure to obtain the transmit signal matrices for perfect and imperfect CSI scenarios is described below.

A. Perfect CSI

For the antipodal signaling scenario with $\mathbf{u}_{k,0} = -\mathbf{u}_k$ and $\mathbf{u}_{k,1} = \mathbf{u}_k$, substituting the expressions for $\mu_{T_{\mathrm{A}}|\mathcal{H}_0}$, $\mu_{T_{\mathrm{A}}|\mathcal{H}_1}$, $\sigma^2_{T_{\mathrm{A}}|\mathcal{H}_0}$ from Theorem 1 in (55), the deflection coefficient $d^2_{\mathrm{A}}(\mathbf{u})$ for $\mathbf{u} = \mathbf{u}_{\mathrm{A}} = \mathrm{vec}(\mathbf{U}_A^T)$, can be determined as

$$\begin{aligned} d^2_{\mathrm{A}}(\mathbf{u}_{\mathrm{A}}) &= \frac{(\mu_{T_{\mathrm{A}}|\mathcal{H}_1} - \mu_{T_{\mathrm{A}}|\mathcal{H}_0})^2}{\sigma^2_{T_{\mathrm{A}}|\mathcal{H}_0}} \\ &= \frac{\big(\sum_{k=1}^{K}\sqrt{p_u}M\beta_k a_k(b_k-c_k)\|\mathbf{u}_k\|^2\big)^2}{\sum_{k=1}^{K}M\beta_k a_k^2\|\mathbf{u}_k\|^2\Big(p_uM\beta_k(1-c_k^2)\|\mathbf{u}_k\|^2 + \frac{\sigma_n^2}{2}\Big)} \\ &= \frac{(\mathbf{u}_{\mathrm{A}}^H\mathbf{\Gamma}_L\mathbf{u}_{\mathrm{A}})^2}{(\mathbf{u}_{\mathrm{A}}^H\mathbf{\Psi}_L\mathbf{u}_{\mathrm{A}})^2 + \mathbf{u}_{\mathrm{A}}^H\mathbf{\Theta}_L\mathbf{u}_{\mathrm{A}}}, \end{aligned} \quad (56)$$

where $\mathbf{\Gamma}_L = \mathbf{\Gamma}\otimes\mathbf{I}_L$, $\mathbf{\Psi}_L = \mathbf{\Psi}\otimes\mathbf{I}_L$, $\mathbf{\Theta}_L = \mathbf{\Theta}\otimes\mathbf{I}_L$ and the matrices $\mathbf{\Gamma}\in\mathbb{C}^{K\times K}$, $\mathbf{\Psi}\in\mathbb{C}^{K\times K}$, $\mathbf{\Theta}\in\mathbb{C}^{K\times K}$ are diagonal, with their principal diagonal elements determined as

$$[\mathbf{\Gamma}]_{k,k}=\sqrt{p_u}M\beta_k a_k(b_k-c_k), [\mathbf{\Psi}]_{k,k}=\sqrt{p_u}M\beta_k a_k\sqrt{1-c_k^2},$$

$$[\mathbf{\Theta}]_{k,k} = \frac{\sigma_n^2}{2}M\beta_k a_k^2. \quad (57)$$

For a detailed proof of the above expressions, the reader is referred to Section I of the technical report in [35]. Since the expression in (56) is non-convex, direct maximization of the deflection coefficient in (56) is difficult to achieve. Therefore, for a tractable solution, the optimization objective can be modified as shown below

$$\text{max. } \frac{\mathbf{u}_{\mathrm{A}}^H(\mathbf{\Gamma}_L\mathbf{u}_{\mathrm{A}}\mathbf{u}_{\mathrm{A}}^H\mathbf{\Gamma}_L)\mathbf{u}_{\mathrm{A}}}{\mathbf{u}_{\mathrm{A}}^H(\mathbf{\Psi}_L\mathbf{u}_{\mathrm{A}}\mathbf{u}_{\mathrm{A}}^H\mathbf{\Psi}_L+\mathbf{\Theta}_L)\mathbf{u}_{\mathrm{A}}} = \text{max. } \frac{\mathbf{u}_{\mathrm{A}}^H\mathbf{\Xi}\mathbf{u}_{\mathrm{A}}}{\mathbf{u}_{\mathrm{A}}^H\mathbf{\Omega}\mathbf{u}_{\mathrm{A}}}, \quad (58)$$

where $\mathbf{\Xi} = \mathbf{\Gamma}_L\mathbf{u}_{\mathrm{A}}\mathbf{u}_{\mathrm{A}}^H\mathbf{\Gamma}_L$, $\mathbf{\Omega} = \mathbf{\Psi}_L\mathbf{u}_{\mathrm{A}}\mathbf{u}_{\mathrm{A}}^H\mathbf{\Psi}_L + \mathbf{\Theta}_L$. It can be observed that the objective function in (58) can be further simplified in a manner similar to the standard form corresponding to a two-way partitioning problem [33] as

$$\begin{aligned} \text{max. } \frac{\mathbf{u}_{\mathrm{A}}^H\mathbf{\Xi}\mathbf{u}_{\mathrm{A}}}{\mathbf{u}_{\mathrm{A}}^H\mathbf{\Omega}^{1/2}\mathbf{\Omega}^{1/2}\mathbf{u}_{\mathrm{A}}} &= \text{max. } \frac{\mathbf{s}_{\mathrm{A}}^H\mathbf{\Omega}^{-1/2}\mathbf{\Xi}\mathbf{\Omega}^{-1/2}\mathbf{s}_{\mathrm{A}}}{\mathbf{s}_{\mathrm{A}}^H\mathbf{s}_{\mathrm{A}}} \\ &= \text{max. } \frac{\mathbf{s}_{\mathrm{A}}^H\mathbf{Q}\mathbf{s}_{\mathrm{A}}}{\mathbf{s}_{\mathrm{A}}^H\mathbf{s}_{\mathrm{A}}}, \end{aligned} \quad (59)$$

where $\mathbf{Q} = \mathbf{\Omega}^{-1/2}\mathbf{\Xi}\mathbf{\Omega}^{-1/2}$ and $\mathbf{s}_{\mathrm{A}} = \mathbf{\Omega}^{1/2}\mathbf{u}_{\mathrm{A}}$. Let $\mathbf{u}_{\mathrm{A}}$ be initialized as $\mathbf{u}_{\mathrm{A}}^{(0)} = \mathrm{vec}\Big(\big(\mathbf{U}_{\mathrm{A}}^{(0)}\big)^T\Big)$, where the matrix $\mathbf{U}_{\mathrm{A}}^{(0)}$ represents a semi-orthogonal matrix at the 0th iteration. Therefore, the iterative optimization problem in the ith iteration to obtain the transmission matrix that further improves the detection performance of the proposed schemes for a massive MIMO WSN can be stated as below.

Theorem 3. *The transmission matrix $\mathbf{U}_A^{(i)}$ for the ith iteration in the distributed detection scenario with perfect CSI and antipodal signaling is given as $\mathbf{U}_A^{(i)} = \Big(vec^{-1}\Big(\big(\mathbf{\Omega}^{(i-1)}\big)^{-1/2}\mathbf{s}_A^{(i)}\Big)\Big)^T$, where $\mathbf{s}_A^{(i)}$ is the solution of the optimization problem below*

$$\max_{\mathbf{s}_A^{(i)}} \ \frac{\mathbf{s}_A^{(i)H}\mathbf{Q}^{(i-1)}\mathbf{s}_A^{(i)}}{\mathbf{s}_A^{(i)H}\mathbf{s}_A^{(i)}}, \quad (60)$$

where $\mathbf{Q}^{(i-1)}=\left(\mathbf{\Omega}^{(i-1)}\right)^{-1/2}\mathbf{\Xi}^{(i-1)}\left(\mathbf{\Omega}^{(i-1)}\right)^{-1/2}$ *and* $\mathbf{s}_A^{(i)}=\left(\mathbf{\Omega}^{(i-1)}\right)^{1/2}\mathbf{u}_A^{(i)}$. *The matrices* $\mathbf{\Xi}^{(i-1)},\mathbf{\Omega}^{(i-1)}$ *are obtained by substituting* $\mathbf{u}_A^{(i-1)}$ *in lieu of* $\mathbf{u}_A$ *in the expression* (58)*.*

The solution of the vector $\mathbf{u}_{\mathrm{A}}^{(i)}$ at the ith iteration is obtained by solving the optimization problem in (60) and is given as $\mathbf{u}_{\mathrm{A}}^{(i)}=\kappa\left(\mathbf{\Omega}^{(i-1)}\right)^{-1/2}\boldsymbol{\nu}^{(i-1)}$, where $\boldsymbol{\nu}^{(i-1)}$ represents the eigenvector of unit length corresponding to the maximum eigenvalue of the matrix $\mathbf{Q}^{(i-1)}$ and κ represents the total power of $\mathbf{u}_{\mathrm{A}}^{(i)}$.

Alternative solution : The solution to the optimization problem in (56) can also be obtained numerically as follows. The epigraph form of the optimization problem is

$$\begin{aligned}&\max_{\mathbf{u}_{\mathrm{A}}^{(i)}}\ \ t\\ &\text{subject to}\ \ d_{\mathrm{A}}^2\left(\mathbf{u}_{\mathrm{A}}^{(i)}\right)\geq t.\end{aligned}\tag{61}$$

Let $\mathbf{u}_{\mathrm{A}}^{(i-1)}$ denote the value of $\mathbf{u}_{\mathrm{A}}$ obtained in the $(i-1)$th iteration. The first order Taylor series approximation of the objective function $d_{\mathrm{A}}^2\left(\mathbf{u}_{\mathrm{A}}^{(i)}\right)$ close to $\mathbf{u}_{\mathrm{A}}^{(i-1)}\in\mathbb{C}^{KL\times 1}$ can be expressed as

$$d_{\mathrm{A}}^2\left(\mathbf{u}_{\mathrm{A}}^{(i)}\right)=d_{\mathrm{A}}^2\left(\mathbf{u}_{\mathrm{A}}^{(i-1)}\right)+\nabla d_{\mathrm{A}}^2\left(\mathbf{u}_{\mathrm{A}}^{(i-1)}\right)^T\left(\mathbf{u}_{\mathrm{A}}^{(i)}-\mathbf{u}_{\mathrm{A}}^{(i-1)}\right),\tag{62}$$

where the expression for gradient $\nabla d_{\mathrm{A}}^2\left(\mathbf{u}_{\mathrm{A}}^{(i-1)}\right)$ is given in (63). The equivalent quadratic constrained linear program to determine the vector $\mathbf{u}_{\mathrm{A}}^{(i)}$ in the ith iteration is

$$\begin{aligned}&\max_{\mathbf{u}_{\mathrm{A}}^{(i)}}\ \ t\\ &\text{subject to}\ \ d_{\mathrm{A}}^2\left(\mathbf{u}_{\mathrm{A}}^{(i)}\right)\geq t\\ &\qquad\quad \mathbf{u}_{\mathrm{A}}^{(i)H}\mathbf{u}_{\mathrm{A}}^{(i)}\leq\kappa,\end{aligned}\tag{64}$$

where κ represents the total beacon power and $d_{\mathrm{A}}^2\left(\mathbf{u}_{\mathrm{A}}^{(i)}\right)$ denotes the first order Taylor series approximation given in (62). The above problem can be solved using a practical convex solver such as CVX [36]. At convergence, the value of $\mathbf{s}_{\mathrm{A}}$ is denoted by $\mathbf{s}_{\mathrm{A}}^*$ from which the vector $\mathbf{u}_{\mathrm{A}}^*$ and the signal matrix $\mathbf{U}_{\mathrm{A}}^*$ can in turn be obtained using the relations mentioned above.

Similarly, for the non-antipodal signaling case where the kth sensor transmit signal vectors are $\mathbf{0},\mathbf{u}_k$, the deflection coefficient $d_{\mathrm{N}}^2(\mathbf{u}_{\mathrm{N}})$ for the test statistic in (32) is simplified as

$$d_{\mathrm{N}}^2(\mathbf{u}_{\mathrm{N}})=\frac{(\mathbf{u}_{\mathrm{N}}^H\check{\mathbf{\Gamma}}_L\mathbf{u}_{\mathrm{N}})^2}{(\mathbf{u}_{\mathrm{N}}^H\check{\mathbf{\Psi}}_L\mathbf{u}_{\mathrm{N}})^2+\mathbf{u}_{\mathrm{N}}^H\check{\mathbf{\Theta}}_L\mathbf{u}_{\mathrm{N}}},\tag{65}$$

where $\check{\mathbf{\Gamma}}$, $\check{\mathbf{\Psi}}$ and $\check{\mathbf{\Theta}}$ represent the diagonal matrices, such that $\check{\mathbf{\Gamma}}_L=\frac{1}{2}\ \mathbf{\Gamma}_L$, $\check{\mathbf{\Psi}}_L=\frac{1}{2}\ \mathbf{\Psi}_L$, $\check{\mathbf{\Theta}}_L=\mathbf{\Theta}_L$ in (65). The transmission matrix $\mathbf{U}_{\mathrm{N}}$ for the non-antipodal signaling scenario can be obtained as the solution of the optimization problem below.

$$\max.\ \ \frac{\mathbf{s}_{\mathrm{N}}^H\check{\mathbf{Q}}\mathbf{s}_{\mathrm{N}}}{\mathbf{s}_{\mathrm{N}}^H\mathbf{s}_{\mathrm{N}}},\tag{66}$$

where $\check{\mathbf{Q}}=\check{\mathbf{\Omega}}^{-1/2}\check{\mathbf{\Xi}}\check{\mathbf{\Omega}}^{-1/2}$ and $\mathbf{s}_{\mathrm{N}}=\check{\mathbf{\Omega}}^{1/2}\mathbf{u}_{\mathrm{N}}$. The solution can be determined via iterative maximization of the cost function above similar to that for the antipodal scenario described in Theorem 3 or the subsequent alternative procedure.

B. Imperfect CSI

The transmission matrices considering CSI uncertainty for distributed detection in massive MIMO WSNs are obtained below. Consider the antipodal signaling scenario with signaling vectors $\mathbf{u}_{k,0}=-\mathbf{u}_k$, $\mathbf{u}_{k,1}=\mathbf{u}_k$ indicating the absence and presence of the signal of interest, respectively. The framework to obtain the signaling matrix is presented next.

Considering the uncertainty in the acquired CSI, the deflection coefficient $d_{\mathrm{R,A}}^2(\mathbf{u}_{\mathrm{R,A}})$ defined in (55), for the test statistic in (44), can be expressed as

$$\begin{aligned}d_{\mathrm{R,A}}^2(\mathbf{u}_{\mathrm{R,A}})&\triangleq\frac{(\mu_{T_{\mathrm{R,A}}|\mathcal{H}_1}-\mu_{T_{\mathrm{R,A}}|\mathcal{H}_0})^2}{\sigma^2_{T_{\mathrm{R,A}}|\mathcal{H}_0}}\\&=\frac{\left(\sum_{k=1}^K\sqrt{p_u}M\tilde{\beta}_k a_k(b_k-c_k)\|\mathbf{u}_k\|^2\right)^2}{\sum_{k=1}^K M\tilde{\beta}_k a_k^2\|\mathbf{u}_k\|^2\left(p_u M\tilde{\beta}_k(1-c_k^2)\|\mathbf{u}_k\|^2+\frac{\sigma_w^2}{2}\right)}\\&=\frac{(\mathbf{u}_{\mathrm{R,A}}^H\check{\mathbf{\Gamma}}_L\mathbf{u}_{\mathrm{R,A}})^2}{(\mathbf{u}_{\mathrm{R,A}}^H\check{\mathbf{\Psi}}_L\mathbf{u}_{\mathrm{R,A}})^2+\mathbf{u}_{\mathrm{R,A}}^H\check{\mathbf{\Theta}}_L\mathbf{u}_{\mathrm{R,A}}},\end{aligned}\tag{67}$$

where $\mu_{T_{\mathrm{R,A}}|\mathcal{H}_0}$, $\mu_{T_{\mathrm{R,A}}|\mathcal{H}_1}$, and $\sigma^2_{T_{\mathrm{R,A}}|\mathcal{H}_0}$ for the test statistic in (44) are given in (47), (48) and (49), respectively. Let $\check{\mathbf{\Gamma}}_L=\check{\mathbf{\Gamma}}\otimes\mathbf{I}_L$, $\check{\mathbf{\Psi}}_L=\check{\mathbf{\Psi}}\otimes\mathbf{I}_L$ and $\check{\mathbf{\Theta}}_L=\check{\mathbf{\Theta}}\otimes\mathbf{I}_L$, where the kth principal diagonal elements of the matrices $\check{\mathbf{\Gamma}}$, $\check{\mathbf{\Psi}}$, and $\check{\mathbf{\Theta}}$ are obtained by replacing β_k by $\tilde{\beta}_k$ and σ_n^2 by σ_w^2 in (57).

The vector $\mathbf{s}_{\mathrm{R,A}}^*$ is obtained via an iterative solution of the cost function given below, similar to that of Theorem 3

$$\max.\ \ \frac{\mathbf{s}_{\mathrm{R,A}}^H\check{\mathbf{Q}}\mathbf{s}_{\mathrm{R,A}}}{\mathbf{s}_{\mathrm{R,A}}^H\mathbf{s}_{\mathrm{R,A}}},\tag{68}$$

where $\check{\mathbf{Q}}=\check{\mathbf{\Omega}}^{-1/2}\check{\mathbf{\Xi}}\check{\mathbf{\Omega}}^{-1/2}$, vector $\mathbf{s}_{\mathrm{R,A}}=\check{\mathbf{\Omega}}^{1/2}\mathbf{u}_{\mathrm{R,A}}\in\mathbb{C}^{KL\times 1}$. The vector $\mathbf{u}_{\mathrm{R,A}}^*$ and the transmit matrix $\mathbf{U}_{\mathrm{R,A}}^*$ are in turn obtained from $\mathbf{s}_{\mathrm{R,A}}^*$ using the relations $\mathbf{u}_{\mathrm{R,A}}^*=\check{\mathbf{\Omega}}^{-1/2}\mathbf{s}_{\mathrm{R,A}}^*$ and $\mathbf{U}_{\mathrm{R,A}}^*=(\mathrm{vec}^{-1}(\mathbf{u}_{\mathrm{R,A}}^*))^T$, respectively.

Along similar lines, the transmission matrix $\mathbf{U}_{\mathrm{R,N}}^*$ for non-antipodal signaling using constellation $\{\mathbf{0},\mathbf{u}_k\}$ under CSI uncertainty can be obtained from $\mathbf{s}_{\mathrm{R,N}}^*$ evaluated as the solution of the optimization problem given as

$$\max.\ \ \frac{\mathbf{s}_{\mathrm{R,N}}^H\tilde{\mathbf{Q}}\mathbf{s}_{\mathrm{R,N}}}{\mathbf{s}_{\mathrm{R,N}}^H\mathbf{s}_{\mathrm{R,N}}},\tag{69}$$

where the matrix $\tilde{\mathbf{Q}}=\tilde{\mathbf{\Omega}}^{-1/2}\tilde{\mathbf{\Xi}}\tilde{\mathbf{\Omega}}^{-1/2}$ and the principal diagonal entries of the diagonal matrices $\tilde{\mathbf{\Gamma}}$, $\tilde{\mathbf{\Psi}}$ and $\tilde{\mathbf{\Theta}}$ are obtained by replacing p_u by $\frac{p_u}{4}$, β_k by $\tilde{\beta}_k$ and σ_n^2 by σ_w^2 in (57). The next section presents the performance analysis for large antenna array in massive MIMO WSN.

VI. Large Array Performance Analysis

The asymptotic system performance of the proposed rules with a very large number of antennas at the FC, i.e., when $M\to\infty$, for the different detection scenarios considered above, is obtained below. The resulting analytical expressions and values for the asymptotic probabilities of detection and false alarm can be compared with their non-asymptotic counterparts determined previously to derive further insights into the system performance.

$$\nabla d_{\mathrm{A}}^2\big(\mathbf{u}_{\mathrm{A}}^{(i-1)}\big)=\frac{\left[4\boldsymbol{\Gamma}_L\mathbf{u}_{\mathrm{A}}\left((\mathbf{u}_{\mathrm{A}}^H\boldsymbol{\Psi}_L\mathbf{u}_{\mathrm{A}})^2+\mathbf{u}_{\mathrm{A}}^H\boldsymbol{\Theta}_L\mathbf{u}_{\mathrm{A}}\right)-(\mathbf{u}_{\mathrm{A}}^H\boldsymbol{\Gamma}_L\mathbf{u}_{\mathrm{A}})\left(4\boldsymbol{\Psi}_L\mathbf{u}_{\mathrm{A}}(\mathbf{u}_{\mathrm{A}}^H\boldsymbol{\Psi}_L\mathbf{u}_{\mathrm{A}})+2\boldsymbol{\Theta}_L\mathbf{u}_{\mathrm{A}}\right)\right]}{(\mathbf{u}_{\mathrm{A}}^H\boldsymbol{\Gamma}_L\mathbf{u}_{\mathrm{A}})^{-1}\left[(\mathbf{u}_{\mathrm{A}}^H\boldsymbol{\Psi}_L\mathbf{u}_{\mathrm{A}})^2+\mathbf{u}_{\mathrm{A}}^H\boldsymbol{\Theta}_L\mathbf{u}_{\mathrm{A}}\right]^2}\Bigg|_{\mathbf{u}_{\mathrm{A}}=\mathbf{u}_{\mathrm{A}}^{(i-1)}}. \quad (63)$$

A. Large Array Performance Analysis under perfect CSI

Consider the power scaling $p_u=\frac{\bar{p}_u}{M}$, where $\bar{p}_u$ is the average transmit power of each sensor. The result below describes the asymptotic performance of the perfect CSI based detector presented in (20) in the limit of $M\to\infty$.

Theorem 4. *The asymptotic probabilities of detection (P_D^a) and false alarm (P_{FA}^a) for the antipodal signaling based test in* (20) *for distributed detection at the FC of the massive MIMO WSN are*

$$P_D^a=\lim_{M\to\infty}Q\left(\frac{\gamma_{AP}}{\sigma_{T_{\mathrm{A}}|\mathcal{H}_1}}-\tilde{\mu}_{T_{\mathrm{A}}|\mathcal{H}_1}\right)=Q\left(\frac{\gamma_{AP}}{\sigma_{T_{\mathrm{A}}|\mathcal{H}_1}}-\tilde{\mu}^a_{T_{\mathrm{A}}|\mathcal{H}_1}\right), \quad (70)$$

$$P_{FA}^a=\lim_{M\to\infty}Q\left(\frac{\gamma_{AP}}{\sigma_{T_{\mathrm{A}}|\mathcal{H}_0}}-\tilde{\mu}_{T_{\mathrm{A}}|\mathcal{H}_0}\right)=Q\left(\frac{\gamma_{AP}}{\sigma_{T_{\mathrm{A}}|\mathcal{H}_0}}-\tilde{\mu}^a_{T_{\mathrm{A}}|\mathcal{H}_0}\right), \quad (71)$$

where $\tilde{\mu}^a_{T_{\mathrm{A}}|\mathcal{H}_0}$, $\tilde{\mu}^a_{T_{\mathrm{A}}|\mathcal{H}_1}$ denote the normalized means corresponding to the null and alternative hypotheses, respectively, which are given as

$$\tilde{\mu}^a_{T_{\mathrm{A}}|\mathcal{H}_0}=\frac{\sum_{k=1}^K\sqrt{\bar{p}_u}a_kc_k\beta_k\|\mathbf{u}_k\|^2}{\sqrt{\sum_{k=1}^K\beta_ka_k^2\|\mathbf{u}_k\|^2\left(\bar{p}_u\beta_k(1-c_k^2)\|\mathbf{u}_k\|^2+\frac{\sigma_n^2}{2}\right)}}, \quad (72)$$

$$\tilde{\mu}^a_{T_{\mathrm{A}}|\mathcal{H}_1}=\frac{\sum_{k=1}^K\sqrt{\bar{p}_u}a_kb_k\beta_k\|\mathbf{u}_k\|^2}{\sqrt{\sum_{k=1}^K\beta_ka_k^2\|\mathbf{u}_k\|^2\left(\bar{p}_u\beta_k(1-b_k^2)\|\mathbf{u}_k\|^2+\frac{\sigma_n^2}{2}\right)}}. \quad (73)$$

Proof: See Appendix C. ∎

Note : The corresponding asymptotic probabilities of detection (P_D^a) and false alarm (P_{FA}^a) for the non-antipodal signaling based test in (32) in the limit $M\to\infty$ are obtained by replacing $\tilde{\mu}_{T_{\mathrm{A}}|\mathcal{H}_0}$, $\tilde{\mu}_{T_{\mathrm{A}}|\mathcal{H}_1}$ with $\tilde{\mu}_{T_{\mathrm{N}}|\mathcal{H}_0}$, $\tilde{\mu}_{T_{\mathrm{N}}|\mathcal{H}_1}$, respectively, which are given as

$$\tilde{\mu}^a_{T_{\mathrm{N}}|\mathcal{H}_0}=\frac{\sum_{k=1}^K\frac{\sqrt{\bar{p}_u}}{2}a_kc_k\beta_k\|\mathbf{u}_k\|^2}{\sqrt{\sum_{k=1}^K\beta_ka_k^2\|\mathbf{u}_k\|^2\left(\frac{\bar{p}_u}{4}\beta_k(1-c_k^2)\|\mathbf{u}_k\|^2+\frac{\sigma_n^2}{2}\right)}}, \quad (74)$$

$$\tilde{\mu}^a_{T_{\mathrm{N}}|\mathcal{H}_1}=\frac{\sum_{k=1}^K\frac{\sqrt{\bar{p}_u}}{2}a_kb_k\beta_k\|\mathbf{u}_k\|^2}{\sqrt{\sum_{k=1}^K\beta_ka_k^2\|\mathbf{u}_k\|^2\left(\frac{\bar{p}_u}{4}\beta_k(1-b_k^2)\|\mathbf{u}_k\|^2+\frac{\sigma_n^2}{2}\right)}}. \quad (75)$$

This can be shown on lines similar to that of Theorem 4. The asymptotic performance with imperfect CSI is detailed next.

B. Large Array Performance Analysis under Imperfect CSI

In practical scenarios, a signification amount of power is utilized by the training symbols that are used to estimate the CSI. Hence, the power scaling of $p_p=\frac{\bar{p}_p}{\sqrt{M}}$ and $p_u=\frac{\bar{p}_u}{\sqrt{M}}$ is considered for training and detection phases, respectively. The probabilities of detection and false alarm in (46) are used to obtain their asymptotic counterparts that are given in the result below.

Theorem 5. *For a given threshold γ_{AI}, the asymptotic performance of the detector in* (44) *with imperfect CSI is characterized by the probabilities of detection (P_D^a) and false alarm (P_{FA}^a) that are determined as*

$$P_D^a=\lim_{M\to\infty}Q\left(\frac{\gamma_{AI}}{\sigma_{T_{R,A}|\mathcal{H}_1}}-\tilde{\mu}_{T_{R,A}|\mathcal{H}_1}\right)=Q\left(\frac{\gamma_{AI}}{\sigma_{T_{R,A}|\mathcal{H}_1}}-\tilde{\mu}^a_{T_{R,A}|\mathcal{H}_1}\right), \quad (76)$$

$$P_{FA}^a=\lim_{M\to\infty}Q\left(\frac{\gamma_{AI}}{\sigma_{T_{R,A}|\mathcal{H}_0}}-\tilde{\mu}_{T_{R,A}|\mathcal{H}_0}\right)=Q\left(\frac{\gamma_{AI}}{\sigma_{T_{R,A}|\mathcal{H}_0}}-\tilde{\mu}^a_{T_{R,A}|\mathcal{H}_0}\right), \quad (77)$$

The quantities $\tilde{\mu}^a_{T_{R,A}|\mathcal{H}_0}$, $\tilde{\mu}^a_{T_{R,A}|\mathcal{H}_1}$ are the normalized means of (44) *for the null and alternative hypotheses as shown below*

$$\tilde{\mu}^a_{T_{R,A}|\mathcal{H}_0}=\frac{\sum_{k=1}^K\bar{p}_p\sqrt{\bar{p}_u}a_kc_k\beta_k^2\|\mathbf{u}_k\|^2}{\sqrt{\sum_{k=1}^K\bar{p}_p\beta_k^2a_k^2\|\mathbf{u}_k\|^2\left(\bar{p}_p\bar{p}_u\beta_k^2(1-c_k^2)\|\mathbf{u}_k\|^2+\frac{\sigma_n^4}{2}\right)}}, \quad (78)$$

$$\tilde{\mu}^a_{T_{R,A}|\mathcal{H}_1}=\frac{\sum_{k=1}^K\bar{p}_p\sqrt{\bar{p}_u}a_kb_k\beta_k^2\|\mathbf{u}_k\|^2}{\sqrt{\sum_{k=1}^K\bar{p}_p\beta_k^2a_k^2\|\mathbf{u}_k\|^2\left(\bar{p}_p\bar{p}_u\beta_k^2(1-b_k^2)\|\mathbf{u}_k\|^2+\frac{\sigma_n^4}{2}\right)}}, \quad (79)$$

with $b_k=2P_{D,k}-1$ and $c_k=2P_{F,k}-1$.

Proof: See Appendix D. ∎

Note : The corresponding performance metrics for the test in (54) with non-antipodal signaling and imperfect CSI are given similar to the antipodal case in Theorem 5 above, with p_u replaced by $\frac{p_u}{4}$. The closed form expressions for the same are explicitly shown below.

$$\tilde{\mu}^a_{T_{\mathrm{R,N}}|\mathcal{H}_0}=\frac{\sum_{k=1}^K\frac{\sqrt{\bar{p}_u}}{2}\bar{p}_pa_kc_k\beta_k^2\|\mathbf{u}_k\|^2}{\sqrt{\sum_{k=1}^K\bar{p}_p\beta_k^2a_k^2\|\mathbf{u}_k\|^2\left(\frac{\bar{p}_u}{4}\bar{p}_p\beta_k^2(1-c_k^2)\|\mathbf{u}_k\|^2+\frac{\sigma_n^4}{2}\right)}}, \quad (80)$$

$$\tilde{\mu}^a_{T_{\mathrm{R,N}}|\mathcal{H}_1}=\frac{\sum_{k=1}^K\frac{\sqrt{\bar{p}_u}}{2}\bar{p}_pa_kb_k\beta_k^2\|\mathbf{u}_k\|^2}{\sqrt{\sum_{k=1}^K\bar{p}_p\beta_k^2a_k^2\|\mathbf{u}_k\|^2\left(\frac{\bar{p}_u}{4}\bar{p}_p\beta_k^2(1-b_k^2)\|\mathbf{u}_k\|^2+\frac{\sigma_n^4}{2}\right)}}. \quad (81)$$

Proof of the above fact follows on lines similar to that of Theorem 5. It is worth noticing from the above analysis that using a large antenna array at the FC results in a significant reduction in the energy consumption of the individual sensors, i.e., proportional to $\frac{1}{M}$ in the perfect CSI scenario and $\frac{1}{\sqrt{M}}$ with CSI uncertainty. This in turn leads to prolonged battery life of the sensor nodes, which is key to reliable operation of the WSN.

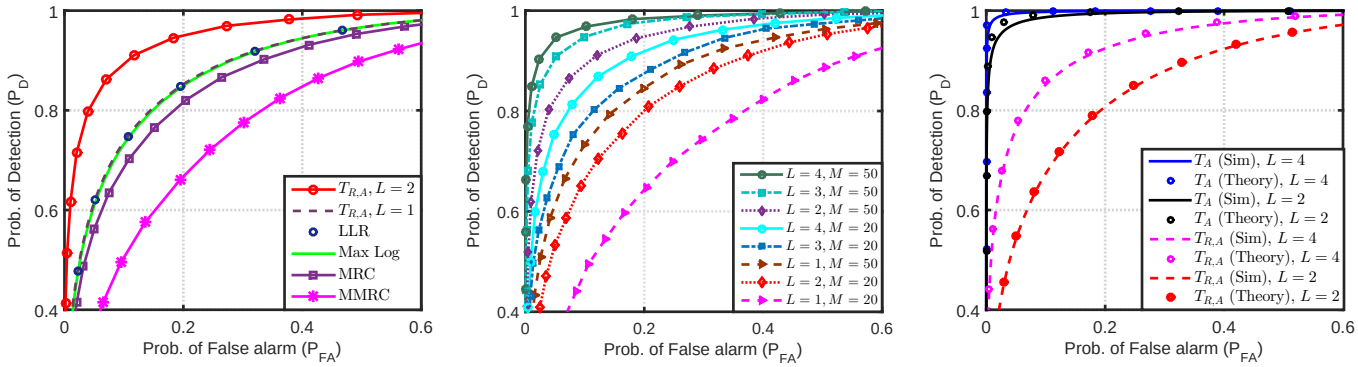

(a) (b) (c)

Fig. 2. Receiver operating characteristic (ROC) plot for comparing (a) Max-Log and MMRC in [28], MRC, LLR with the proposed detector (44) for $M = 50$ antennas, $K = 12$ sensors, $L \in \{1, 2\}$ and at SNR $p_u = -18$ dB. (b) proposed detector in (44) for $M \in \{20, 50\}$ antennas, $K = 12$ sensors, $L \in \{1, 2, 3, 4\}$ and at SNR $p_u = -18$ dB. (c) theoretical and simulation performance of the detectors under perfect CSI in (20) and imperfect CSI in (44) with $K = 12$ sensors, $L \in \{2, 4\}$ and SNR $p_u = -18$ dB.

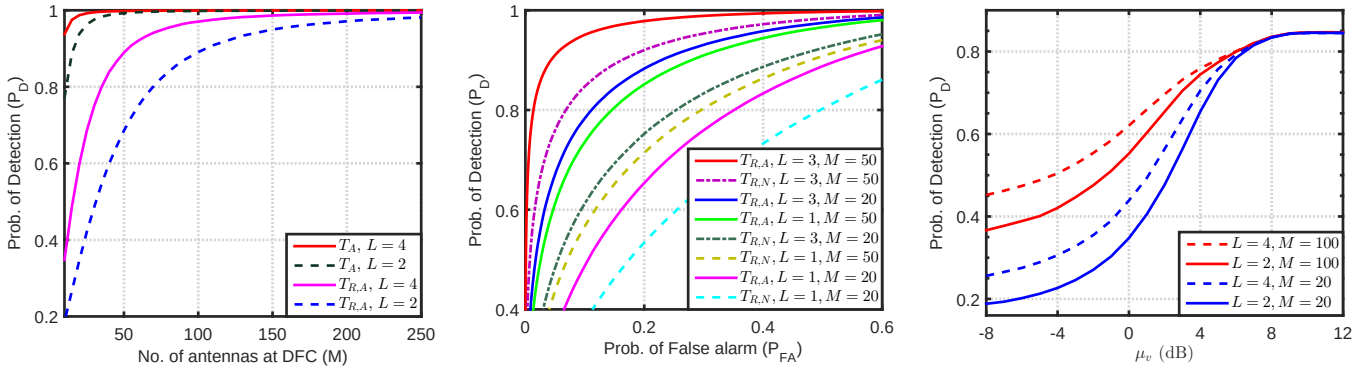

(a) (b) (c)

Fig. 3. (a) P_D vs. M for perfect and imperfect CSI scenarios, $P_{FA} = .01$, for a WSN with $K = 12$ sensors, $L \in \{2, 4\}$ and SNR $p_u = -18$ dB. (b) ROC plot for comparing antipodal and non-antipodal signaling, for a WSN with $K = 12$ sensors, $L \in \{1, 3\}$, $M \in \{20, 50\}$ and SNR $p_u = -18$ dB. (c) P_D vs. μ_v for imperfect CSI scenario using detector $T_{\mathrm{R,A}}(\tilde{\mathbf{Z}})$, $P_{FA} = .01$, for a WSN with $K = 12$ sensors, $L \in \{2, 4\}$ and $M \in \{20, 100\}$.

VII. Detection Performance Analysis

The probability of error expressions for the various distributed detectors described above can be obtained as follows. Let $\Pr(\mathcal{H}_i|\mathcal{H}_j)$ denote the conditional probability of deciding hypothesis $\mathcal{H}_i$ when hypothesis $\mathcal{H}_j$ is true and $\Pr(\mathcal{H}_i)$ represent the prior probability of hypothesis $\mathcal{H}_i$, where $i, j \in \{0, 1\}$. Hence, the resulting probability of error can be expressed as [34]

$$P_e = \Pr(\mathcal{H}_0|\mathcal{H}_1)\Pr(\mathcal{H}_1) + \Pr(\mathcal{H}_1|\mathcal{H}_0)\Pr(\mathcal{H}_0). \quad (82)$$

Let the prior probabilities corresponding to the null and alternative hypotheses take values $\Pr(\mathcal{H}_0) = 1-\zeta$ and $\Pr(\mathcal{H}_1) = \zeta$. The conditional probabilities $\Pr(\mathcal{H}_0|\mathcal{H}_1)$, $\Pr(\mathcal{H}_1|\mathcal{H}_0)$, can be written in terms of the system probabilities of detection P_D and false alarm P_{FA} as $\Pr(\mathcal{H}_0|\mathcal{H}_1) = (1 - P_D)$ and $\Pr(\mathcal{H}_1|\mathcal{H}_0) = P_{FA}$, respectively. Therefore, the expression for P_e in (82) reduces to

$$P_e = \zeta(1 - P_D) + (1 - \zeta)P_{FA}. \quad (83)$$

Hence, using the result in Theorem 1, the probability of error for the perfect CSI based test in (20) can be readily derived as

$$P_e = \zeta\left(1 - Q\left(\frac{\gamma_{\mathrm{AP}} - \mu_{T_{\mathrm{A}}|\mathcal{H}_1}}{\sigma_{T_{\mathrm{A}}|\mathcal{H}_1}}\right)\right) + (1-\zeta)\,Q\left(\frac{\gamma_{\mathrm{AP}} - \mu_{T_{\mathrm{A}}|\mathcal{H}_0}}{\sigma_{T_{\mathrm{A}}|\mathcal{H}_0}}\right), \quad (84)$$

where $\mu_{T_{\mathrm{A}}|\mathcal{H}_0}$, $\mu_{T_{\mathrm{A}}|\mathcal{H}_1}$, $\sigma^2_{T_{\mathrm{A}}|\mathcal{H}_0}$ and $\sigma^2_{T_{\mathrm{A}}|\mathcal{H}_1}$ are as defined therein. Similarly, the probability of error for the test statistic in (44) under imperfect CSI with antipodal signaling is given as,

$$P_e = \zeta\left(1 - Q\left(\frac{\gamma_{\mathrm{AI}} - \mu_{T_{\mathrm{R,A}}|\mathcal{H}_1}}{\sigma_{T_{\mathrm{R,A}}|\mathcal{H}_1}}\right)\right) + (1-\zeta)\,Q\left(\frac{\gamma_{\mathrm{AI}} - \mu_{T_{\mathrm{R,A}}|\mathcal{H}_0}}{\sigma_{T_{\mathrm{R,A}}|\mathcal{H}_0}}\right), \quad (85)$$

where the quantities γ_{AI}, $\mu_{T_{\mathrm{R,A}}|\mathcal{H}_0}$, $\mu_{T_{\mathrm{R,A}}|\mathcal{H}_1}$, $\sigma^2_{T_{\mathrm{R,A}}|\mathcal{H}_0}$ and $\sigma^2_{T_{\mathrm{R,A}}|\mathcal{H}_1}$ are determined as in Theorem 2. A similar procedure can be utilized to obtain the probabilities of error for the non-antipodal signaling based tests in (32)/(54), corresponding to perfect and imperfect CSI scenarios, respectively. Simulation results to validate the performance of the proposed schemes are presented next.

VIII. Simulation Results

This section presents simulation results to compare the performance of the proposed detectors for the massive MIMO WSN in (20), (32), (44) and (54) with the conventional schemes, namely the optimal log-likelihood ratio (LLR), standard maximal ratio combiner (MRC), Max-Log and modified maximal ratio combiner (MMRC) detectors described in [28]. The detectors proposed in [28] are based on BPSK modulation at the sensors to transmit their local decisions to the FC.

A brief overview of the detectors proposed in [28] is as follows. The optimal LLR rule maximizes the probability of detection for a given probability of false alarm, employing the NP criterion. The Max-Log detector is obtained by linear filtering the received signal, followed by the use of standard Max-Log approximation used in turbo decoders. The MRC rule is derived using a low-SNR approximation of the LLR obtained under the assumption of perfect sensor decisions, i.e., $\Pr(\mathbf{x} = \mathbf{1}_K|\mathcal{H}_1) = \Pr(\mathbf{x} = -\mathbf{1}_K|\mathcal{H}_0) = 1$. Finally, the MMRC detector is a variation of the MRC detector obtained by removing the dependency on the large-scale fading coefficients.

For simulations, the sensors are assumed to be uniformly distributed in an annular area around the FC, such that the sensors are between the maximum and minimum distances of $r_m = 1000$ meters and $r_c = 100$ meters from the FC, respectively. A total of $K = 12$ sensors are considered and their local performance metrics, i.e., $P_{D,k}$ and $P_{F,k}$, are assumed to be uniformly distributed in $[0.95, 0.40]$ and $[0.01, 0.12]$, respectively. The large-scale fading coefficients are modeled as $\beta_k = v_k/(r_k/r_c)^\alpha$, similar to [6]. Furthermore, the random variable v_k follows the log-normal distribution, i.e. $10\log_{10} v_k \sim \mathcal{N}(\mu_v, \sigma_v^2)$, with μ_v and σ_v denoting the mean and standard deviation, respectively, r_k denoting the distance between the kth sensor and the FC and α representing the path-loss exponent. These parameters are set as $\mu_v = 4$ dB, $\sigma_v = 2$ dB and $\alpha = 2$ [28]. For channel estimation, the minimum length of the pilot symbols required, i.e. $\tau_p = K$, is utilized [6].

Fig. 2a plots the probability of detection (P_D) versus the probability of false alarm (P_{FA}) of the proposed detector in (44) for $L = \{1, 2\}$. It is observed that the proposed scheme yields an improved performance in comparison to the schemes presented in [28]. Moreover, the performance of the proposed detector for $L = 1$ is similar to that of the Max-Log detector and the LLR test. Fig. 2b shows the performance of the proposed detector in Section IV-A for imperfect CSI for different values of transmit vector size $L \in \{1, 2, 3, 4\}$. It is clear that better detection performance is achieved with an increase in L. This improvement is achieved as a consequence of the multiple signaling intervals utilized by the sensing nodes to transmit their local decisions. Subsequently, employing the transmission matrix determined in Section V leads to a further improvement in the detection performance. Moreover, an increase in the number of antennas at the FC leads to a remarkable improvement in the detection performance, demonstrating the advantage of employing a massive antenna array at the FC.

Fig. 2c compares the numerical results based on theoretical expressions of probabilities of detection and false alarm obtained in Theorem 1 and Theorem 2 with their simulation counterparts. It is evident from the figure that they are in close agreement. Fig. 3a plots the probability of detection (P_D) versus the number of antennas M at the FC for a fixed $P_{FA} = 0.01$, for the scenarios with and without CSI uncertainty. The trend shows a significant improvement in the detection performance with increasing number of FC antennas. Fig. 3b compares the probability of detection (P_D) versus the probability of false alarm (P_{FA}) of the proposed detectors in (44) and (54) for both the antipodal and non-antipodal signaling schemes, which clearly demonstrates the benefit of employing the antipodal signaling scheme over the non-antipodal counterpart. In addition, all the proposed detectors are seen to benefit with an increase in the number of FC antennas.

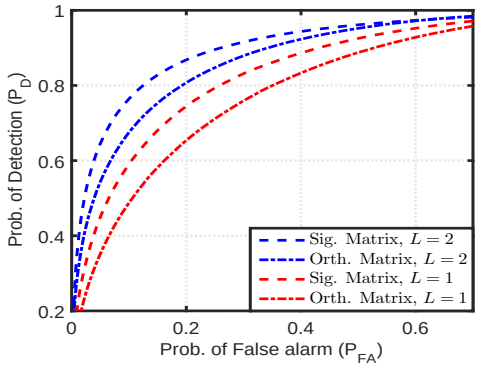

Fig. 4. ROC plot for comparing detectors $T_{\mathrm{R,A}}(\tilde{\mathbf{Z}})$ with orthogonal and signaling matrix obtained in Section V for imperfect CSI scenario, for a WSN with $K = 12$ sensors, $L \in \{1, 2\}$, $M = 20$ and SNR $p_u = -18$ dB.

In Fig. 3c, the probability of detection (P_D) is plotted as a function of μ_v to characterize performance improvement. It is clear that the proposed detector with higher values of L has a lower performance loss in comparison to the ones which employ shorter decision vectors. Fig. 4 compares the receiver operating characteristics of the proposed schemes for the transmission matrix described in Section V for the imperfect CSI scenario. It can be readily inferred that employing the deflection-coefficient based transmission matrix leads to a significantly improved detection performance. Fig. 5a, 5b and 5c show the large antenna performance of the proposed detectors in (20) and (44). For the scenario with perfect CSI, the power is assumed to scale as $p_u = \frac{\bar{p}_u}{M}$, while for the imperfect CSI scenario, this is set as $p_p = \frac{\bar{p}_p}{\sqrt{M}}$ in the training phase and $p_u = \frac{\bar{p}_u}{\sqrt{M}}$ in the reporting phase. It can be noticed that the proposed detectors converge to their corresponding theoretical expressions derived in Theorem 4 and Theorem 5, respectively, thus validating the analytical findings. Fig. 6 plots the probability of error as a function of p_u for a fixed $P_{FA} = 0.001$, for both perfect and imperfect CSI scenarios and compares them with the theoretical results. It is observed that the probability of error decreases with an increase in the SNR. Moreover, the simulated probability of error plots are in close agreement with the theoretical findings.

IX. Conclusion

This paper proposed and investigated the performance of various schemes for distributed detection for a multiple observation vector model in a massive MIMO WSN. Simplified fusion rules for low communication SNR scenarios were determined based on the NP criterion considering also the local detection performance of the individual sensors, for various scenarios, such as with perfect/ imperfect CSI and for antipodal/ non-antipodal signaling. Closed-form expressions were derived to characterize the probabilities of detection P_D

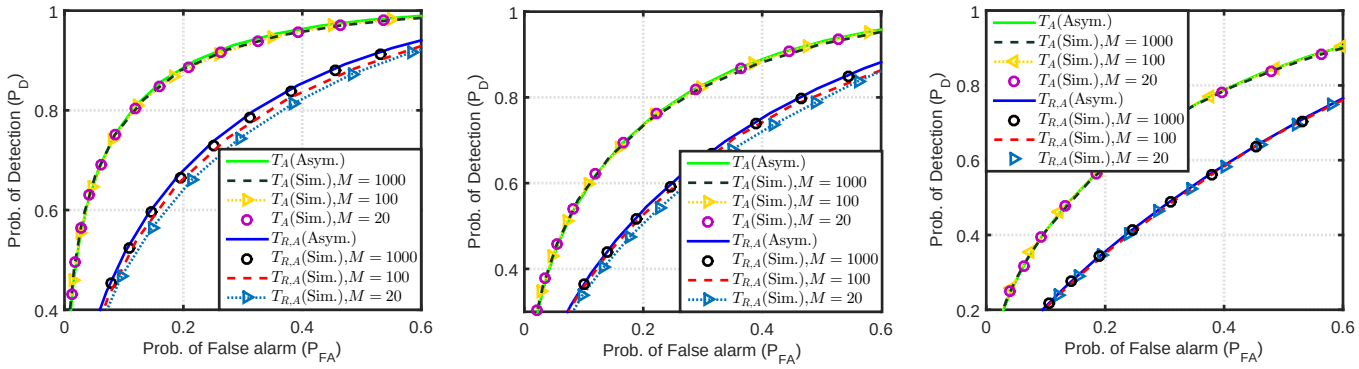

(a) (b) (c)

Fig. 5. Large M performance analysis for (a) proposed detector (20) and (44) for $M \in \{20, 100, 1000\}$ antennas, $K = 12$ sensors, $L = 4$ and at SNR $p_u = -15$ dB. (b) proposed detector (20) and (44) for $M \in \{20, 100, 1000\}$ antennas, $K = 12$ sensors, $L = 2$ and at SNR $p_u = -15$ dB. (c) proposed detector (20) and (44) for $M \in \{20, 100, 1000\}$ antennas, $K = 12$ sensors, $L = 2$ and at SNR $p_u = -18$ dB.

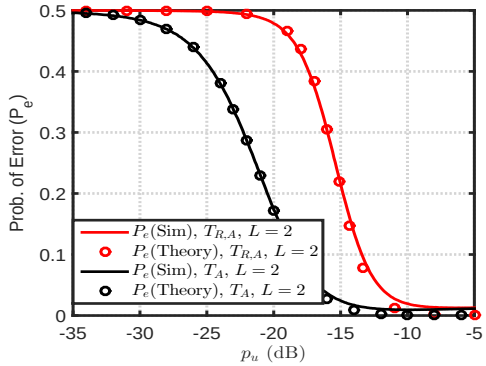

Fig. 6. P_e vs. p_u for perfect and imperfect CSI scenarios using detectors T_A and $T_{R,A}$, respectively, for a WSN with $K = 12$ sensors, $L = 2$ and $M = 20$.

and false alarm P_{FA} as well as the signaling matrices to further enhance detection performance. Further, asymptotic performance upper bounds and the pertinent power scaling laws were obtained via a large antenna array analysis for the detection performance at the FC. Simulation results demonstrated the improved performance of the proposed detectors in comparison to existing schemes such as Max-Log, MRC and MMRC. In the future, this framework can be extended to a scenario with multiple FCs, each equipped with a massive antenna array, to examine the effect of pilot contamination. Furthermore, the problem of sensing of different parameters with correlated sensor observations and sensor selection can be considered.

Appendix A
Fusion rule with Zero Forcing processing

Using the filter matrix $\mathbf{A} = \mathbf{G}(\mathbf{G}^H\mathbf{G})^{-1}$, the system model in (13) can be equivalently reframed as

$$\check{\mathbf{z}}_k = M\Big[\big(\mathbf{A}^H\mathbf{y}(1)\big)_k \dots \big(\mathbf{A}^H\mathbf{y}(L)\big)_k\Big]^T = \sqrt{p_u}M\mathbf{x}_k + \check{\mathbf{n}}_k, \quad (86)$$

where $\check{\mathbf{z}}_k$ follows the Gaussian distribution as $\check{\mathbf{z}}_k \sim \mathcal{CN}(\sqrt{p_u}M\mathbf{x}_k, M\sigma_n^2\beta_k^{-1}\mathbf{I}_L)$. Employing the similar procedure as done for the matched filtering in (15), the test statistic for antipodal signaling under low SNR conditions reduces to $T_A(\check{\mathbf{Z}}) = \sum_{k=1}^{K} a_k\Re(\check{\mathbf{z}}_k^H\mathbf{u}_k)$.

Appendix B
Proof of Theorem 1

The mean of the test statistic in (44) corresponding to the null hypothesis $\mathcal{H}_0$ is given as

$$\begin{aligned}\mu_{T_{\mathrm{R,A}}|\mathcal{H}_0} &= \sum_{k=1}^{K} a_k\Re\Big(\mathbb{E}\big\{(\tilde{\mathbf{z}}_k^H\mathbf{u}_k)|\mathcal{H}_0\big\}\Big)\\ &= \sum_{k=1}^{K} a_k\Re\big(\sqrt{p_u}M\tilde{\beta}_k\mathbb{E}\{\mathbf{x}_k^H|\mathcal{H}_0\}\mathbf{u}_k\big)\\ &= \sum_{k=1}^{K} a_k\Re\Big(\sqrt{p_u}M\tilde{\beta}_k\big(\mathbf{u}_k^H P_{F,k} - \mathbf{u}_k^H(1-P_{F,k})\big)\mathbf{u}_k\Big)\\ &= \sum_{k=1}^{K} \sqrt{p_u}a_k c_k M\tilde{\beta}_k\|\mathbf{u}_k\|^2. \end{aligned} \quad (87)$$

The mean $\mu_{T_{\mathrm{R,A}}|\mathcal{H}_1}$ corresponding to the test statistic for hypothesis $\mathcal{H}_1$ can be derived similarly. The variance $\sigma^2_{T_{\mathrm{R,A}}|\mathcal{H}_0}$ of the test statistic for hypothesis $\mathcal{H}_0$ can be expressed as

$$\sigma^2_{T_{\mathrm{R,A}}|\mathcal{H}_0} = \mathbb{E}\{T^2_{\mathrm{R,A}}(\tilde{\mathbf{Z}})|\mathcal{H}_0\} - \big(\mathbb{E}\{T_{\mathrm{R,A}}(\tilde{\mathbf{Z}})|\mathcal{H}_0\}\big)^2, \quad (88)$$

wherein the first term can be determined as

$$\begin{aligned}\mathbb{E}\{T^2_{\mathrm{R,A}}(\mathbf{Z})|\mathcal{H}_0\} &= \mathbb{E}\Big\{\Big[\sum_{k=1}^{K} a_k\Re\{\tilde{\mathbf{z}}_k^H\mathbf{u}_k\}\Big]^2\Big|\mathcal{H}_0\Big\}\\ &= \sum_{k=1}^{K}\mathbb{E}\Big\{a_k^2\big[\Re\{\sqrt{p_u}M\tilde{\beta}_k\mathbf{x}_k^H\mathbf{u}_k + \tilde{\mathbf{w}}_k^H\mathbf{u}_k\}\big]^2\Big|\mathcal{H}_0\Big\}\\ &= \sum_{k=1}^{K}\Big(p_u M^2\tilde{\beta}_k^2 a_k^2\|\mathbf{u}_k\|^4 + M\tilde{\beta}_k a_k^2\|\mathbf{u}_k\|^2\frac{\sigma_w^2}{2}\Big). \end{aligned} \quad (89)$$

The final expression of variance $\sigma^2_{T_{\mathrm{R,A}}|\mathcal{H}_0}$ in (49) is obtained by utilizing the mean obtained in (87) and the above expression in (89). The variance $\sigma^2_{T_{\mathrm{R,A}}|\mathcal{H}_1}$ for the alternative hypothesis $\mathcal{H}_1$ in (50) can be derived similarly.

Appendix C
Proof of Theorem 4

Under antipodal signaling, the PDF of the test statistic (20) corresponding to the hypothesis $\mathcal{H}_i$ is $T_{\mathrm{A}}(\mathbf{Z}) \sim \mathcal{N}(\mu_{T_{\mathrm{A}}|\mathcal{H}_i}, \sigma^2_{T_{\mathrm{A}}|\mathcal{H}_i})$ which can be scaled to obtain the

equivalent test statistic with unity variance as $\tilde{T}_{\mathrm{A}}(\mathbf{Z}) \sim \mathcal{N}(\tilde{\mu}_{T_{\mathrm{A}}|\mathcal{H}_i}, 1)$, where the new mean $\tilde{\mu}_{T_{\mathrm{A}}|\mathcal{H}_i}$ is defined as

$$\tilde{\mu}_{T_{\mathrm{A}}|\mathcal{H}_i} \triangleq \frac{\mu_{T_{\mathrm{A}}|\mathcal{H}_i}}{\sigma_{T_{\mathrm{A}}|\mathcal{H}_i}}, \quad \text{where } i \in \{0,1\}. \tag{90}$$

From (23) and (25), the above mean $\tilde{\mu}_{T_{\mathrm{A}}|\mathcal{H}_i}$, for $i=0$, is

$$\tilde{\mu}_{T_{\mathrm{A}}|\mathcal{H}_0} = \frac{\sum_{k=1}^{K} \sqrt{p_u} a_k c_k M \beta_k \|\mathbf{u}_k\|^2}{\sqrt{\sum_{k=1}^{K} M \beta_k a_k^2 \|\mathbf{u}_k\|^2 \left(p_u M \beta_k (1-c_k^2) \|\mathbf{u}_k\|^2 + \frac{\sigma_n^2}{2} \right)}}.$$

In the limit case of $M \to \infty$ and using $p_u = \frac{\bar{p}_u}{M}$, the above expression reduces as

$$\tilde{\mu}^{a}_{T_{\mathrm{A}}|\mathcal{H}_0} = \lim_{M\to\infty} \tilde{\mu}_{T_{\mathrm{A}}|\mathcal{H}_0}\Big|_{p_u=\frac{\bar{p}_u}{M}} = \lim_{M\to\infty} \frac{\mu_{T_{\mathrm{A}}|\mathcal{H}_0}}{\sigma_{T_{\mathrm{A}}|\mathcal{H}_0}}\Big|_{p_u=\frac{\bar{p}_u}{M}}$$

$$= \lim_{M\to\infty} \frac{\sum_{k=1}^{K} \sqrt{\frac{\bar{p}_u}{M}} a_k c_k M \beta_k \|\mathbf{u}_k\|^2}{\sqrt{\sum_{k=1}^{K} M \beta_k a_k^2 \|\mathbf{u}_k\|^2 \left(\frac{\bar{p}_u}{M} M \beta_k (1-c_k^2) \|\mathbf{u}_k\|^2 + \frac{\sigma_n^2}{2} \right)}},$$

to obtain (72). Similarly, for hypothesis $\mathcal{H}_1$, the normalized mean in (73) follows by replacing c_k by b_k in the expression above and considering the limit as $M \to \infty$. It can be noted that the last step above employs the assumption $M >> K$, i.e., $K/M \to 0$, similar to standard works such as [5], [6], [28]. When $K/M \to \eta$, where η is a constant, or $K/M \to \infty$, then the interference between the sensors dominates the signal after linear processing, i.e., in (11) and when (38) is multiplied by $\hat{\mathbf{G}}^H$, in the massive MIMO system. Hence, the resulting performance tends to that of a trivial detector with $P_D = 1/2$ and $P_{FA} = 1/2$.

Appendix D
Proof of Theorem 5

The normalized mean for the test statistic in (44) can be determined using (47) and (49) as

$$\tilde{\mu}_{T_{\mathrm{R,A}}|\mathcal{H}_0} = \frac{\sum_{k=1}^{K} \sqrt{p_u} a_k c_k M \tilde{\beta}_k \|\mathbf{u}_k\|^2}{\sqrt{\sum_{k=1}^{K} M \tilde{\beta}_k a_k^2 \|\mathbf{u}_k\|^2 \left(p_u M \tilde{\beta}_k (1-c_k^2) \|\mathbf{u}_k\|^2 + \frac{\sigma_w^2}{2} \right)}}. \tag{91}$$

Substituting $p_u = \frac{\bar{p}_u}{\sqrt{M}}, p_p = \frac{\bar{p}_p}{\sqrt{M}}$ in the above expression for $\tilde{\mu}_{T_{\mathrm{R,A}}|\mathcal{H}_0}$, which on considering the limiting value as $M \to \infty$ yields the expression for the asymptotic normalized mean in (92) to obtain (78). The corresponding expression for $\tilde{\mu}^{a}_{T_{\mathrm{R,A}}|\mathcal{H}_1}$ in (79) can be determined similarly starting with the expressions for $\mu_{T_{\mathrm{R,A}}|\mathcal{H}_1}$, $\sigma^2_{T_{\mathrm{R,A}}|\mathcal{H}_1}$ given in (48), (50), respectively.

References

[1] A. Chawla, A. Patel, A. K. Jagannatham, and P. K. Varshney, "Robust Distributed Detection in Massive MIMO Wireless Sensor Networks under CSI Uncertainty," in *IEEE 88th Veh. Technol. Conf.*, Aug. 2018, pp. 1–5.

[2] F. Rusek, D. Persson, B. K. Lau, E. G. Larsson, T. L. Marzetta, O. Edfors, and F. Tufvesson, "Scaling Up MIMO: Opportunities and Challenges with Very Large Arrays," *IEEE Signal Process. Mag.*, vol. 30, no. 1, pp. 40–60, Jan. 2013.

[3] E. G. Larsson, O. Edfors, F. Tufvesson, and T. L. Marzetta, "Massive MIMO for next generation wireless systems," *IEEE Commun. Mag.*, vol. 52, no. 2, pp. 186–195, Feb. 2014.

[4] D. Gesbert, M. Kountouris, R. W. H. Jr., C. b. Chae, and T. Salzer, "Shifting the MIMO Paradigm," *IEEE Signal Process. Mag.*, vol. 24, no. 5, pp. 36–46, Sep. 2007.

[5] T. L. Marzetta, "Noncooperative Cellular Wireless with Unlimited Numbers of Base Station Antennas," *IEEE Trans. Wireless Commun.*, vol. 9, no. 11, pp. 3590–3600, Nov. 2010.

[6] H. Q. Ngo, E. G. Larsson, and T. L. Marzetta, "Energy and Spectral Efficiency of Very Large Multiuser MIMO Systems," *IEEE Trans. Commun.*, vol. 61, no. 4, pp. 1436–1449, Apr. 2013.

[7] R. Viswanathan and P. K. Varshney, "Distributed detection with multiple sensors I. Fundamentals," *Proc. of the IEEE*, vol. 85, no. 1, pp. 54–63, Jan. 1997.

[8] Z. Chair and P. K. Varshney, "Optimal data fusion in multiple sensor detection systems," *IEEE Trans. Aerosp. Electron. Syst.*, vol. AES-22, no. 1, pp. 98–101, Jan. 1986.

[9] R. Jiang, S. Misra, B. Chen, and A. Swami, "Robust suboptimal decision fusion in wireless sensor networks," in *MILCOM 2005 - 2005 IEEE Mil. Commun. Conf.*, Oct. 2005, pp. 2107–2113 Vol. 4.

[10] R. Niu, B. Chen, and P. K. Varshney, "Fusion of decisions transmitted over Rayleigh fading channels in wireless sensor networks," *IEEE Trans. Signal Process.*, vol. 54, no. 3, pp. 1018–1027, Mar. 2006.

[11] B. Chen, L. Tong, and P. K. Varshney, "Channel-aware distributed detection in wireless sensor networks," *IEEE Signal Process. Mag.*, vol. 23, no. 4, pp. 16–26, Jul. 2006.

[12] J. Chamberland and V. V. Veeravalli, "Wireless Sensors in Distributed Detection Applications," *IEEE Signal Process. Mag.*, vol. 24, no. 3, pp. 16–25, May 2007.

[13] W. Li and H. Dai, "Distributed detection in wireless sensor networks using a multiple access channel," *IEEE Trans. Signal Process.*, vol. 55, no. 3, pp. 822–833, Mar. 2007.

[14] C. R. Berger, M. Guerriero, S. Zhou, and P. Willett, "PAC vs. MAC for Decentralized Detection Using Noncoherent Modulation," *IEEE Trans. Signal Process.*, vol. 57, no. 9, pp. 3562–3575, Sep. 2009.

[15] D. Ciuonzo and G. Romano and P. Salvo Rossi, "Optimality of Received Energy in Decision Fusion Over Rayleigh Fading Diversity MAC With Non-Identical Sensors," *IEEE Trans. Signal Process.*, vol. 61, no. 1, pp. 22–27, Jan. 2013.

[16] X. Zhang, H. V. Poor, and M. Chiang, "Optimal Power Allocation for Distributed Detection Over MIMO Channels in Wireless Sensor Networks," *IEEE Trans. Signal Process.*, vol. 56, no. 9, pp. 4124–4140, Sep. 2008.

[17] A. Patel, S. Biswas, and A. K. Jagannatham, "Multiple Beacon Based Robust Cooperative Spectrum Sensing in MIMO Cognitive Radio Networks," in *IEEE 78th Veh. Technol. Conf.*, Sep. 2013, pp. 1–5.

[18] A. Patel, H. Ram, A. K. Jagannatham, and P. K. Varshney, "Robust Cooperative Spectrum Sensing for MIMO Cognitive Radio Networks Under CSI Uncertainty," *IEEE Trans. Signal Process.*, vol. 66, no. 1, pp. 18–33, Jan. 2018.

[19] Q. Cheng, B. Chen, and P. K. Varshney, "Detection performance limits for distributed sensor networks in the presence of nonideal channels," *IEEE Trans. Wireless Commun.*, vol. 5, no. 11, pp. 3034–3038, Nov. 2006.

[20] D. Ciuonzo and G. Romano and P. Salvo Rossi, "Channel-Aware Decision Fusion in Distributed MIMO Wireless Sensor Networks: Decode-and-Fuse vs. Decode-then-Fuse," *IEEE Trans. Wireless Commun.*, vol. 11, no. 8, pp. 2976–2985, Aug. 2012.

[21] M. K. Banavar, A. D. Smith, C. Tepedelenlioglu, and A. Spanias, "On the Effectiveness of Multiple Antennas in Distributed Detection over Fading MACs," *IEEE Trans. Wireless Commun.*, vol. 11, no. 5, pp. 1744–1752, May 2012.

[22] I. Nevat, G. W. Peters, and I. B. Collings, "Distributed Detection in Sensor Networks Over Fading Channels With Multiple Antennas at the Fusion Centre," *IEEE Trans. Signal Process.*, vol. 62, no. 3, pp. 671–683, Feb. 2014.

[23] F. Jiang, J. Chen, and A. L. Swindlehurst, "Estimation in phase-shift and forward wireless sensor networks," *IEEE Trans. Signal Process.*, vol. 61, no. 15, pp. 3840–3851, Aug. 2013.

[24] M. K. Banavar, A. D. Smith, C. Tepedelenliolu, and A. Spanias, "Distributed detection over fading macs with multiple antennas at the fusion center," in *2010 IEEE Int. Conf. Acoust., Speech, Signal Process.*, Mar. 2010, pp. 2894–2897.

[25] F. Jiang, J. Chen, A. L. Swindlehurst, and J. A. Lpez-Salcedo, "Massive MIMO for Wireless Sensing With a Coherent Multiple Access Channel," *IEEE Trans. Signal Process.*, vol. 63, no. 12, pp. 3005–3017, Jun. 2015.

$$\tilde{\mu}^{a}_{T_{\mathrm{R,A}}|\mathcal{H}_0}=\lim_{M\to\infty}\frac{\sum_{k=1}^{K}\frac{\sqrt{\bar{p}_u}}{M^{1/4}}a_k c_k M\frac{\frac{\bar{p}_p}{\sqrt{M}}\beta_k^2}{\sigma_n^2+\frac{\bar{p}_p}{\sqrt{M}}\beta_k}\|\mathbf{u}_k\|^2}{\sqrt{\sum_{k=1}^{K}M\frac{\frac{\bar{p}_p}{\sqrt{M}}\beta_k^2}{\sigma_n^2+\frac{\bar{p}_p}{\sqrt{M}}\beta_k}a_k^2\|\mathbf{u}_k\|^2\left(\frac{\bar{p}_u}{\sqrt{M}}M\frac{\frac{\bar{p}_p}{\sqrt{M}}\beta_k^2}{\sigma_n^2+\frac{\bar{p}_p}{\sqrt{M}}\beta_k}(1-c_k^2)\|\mathbf{u}_k\|^2+\frac{1}{2}\left(\frac{\bar{p}_u}{\sqrt{M}}\sum_{k=1}^{K}|u_{k,i}(l)|^2\frac{\sigma_n^2\beta_k}{\sigma_n^2+\frac{\bar{p}_p}{\sqrt{M}}\beta_k}+\sigma_n^2\right)\right)}}, \quad (92)$$

[26] A. Shirazinia and S. Dey and D. Ciuonzo and P. Salvo Rossi, "Massive MIMO for Decentralized Estimation of a Correlated Source," *IEEE Trans. Signal Process.*, vol. 64, no. 10, pp. 2499–2512, May 2016.

[27] G. Ding, X. Gao, Z. Xue, Y. Wu, and Q. Shi, "Massive MIMO for Distributed Detection With Transceiver Impairments," *IEEE Trans. Veh. Technol.*, vol. 67, no. 1, pp. 604–617, Jan. 2018.

[28] D. Ciuonzo and P. Salvo Rossi and S. Dey, "Massive MIMO Channel-Aware Decision Fusion," *IEEE Trans. Signal Process.*, vol. 63, no. 3, pp. 604–619, Feb. 2015.

[29] D. Ciuonzo, A. Aubry, and V. Carotenuto, "Rician MIMO Channel- and Jamming-Aware Decision Fusion," *IEEE Trans. Signal Process.*, vol. 65, no. 15, pp. 3866–3880, Aug. 2017.

[30] A. Chockalingam and B. S. Rajan, *Large MIMO Systems*. Cambridge University Press, 2014.

[31] B. Chen, R. Jiang, T. Kasetkasem, and P. K. Varshney, "Channel aware decision fusion in wireless sensor networks," *IEEE Trans. Signal Process.*, vol. 52, no. 12, pp. 3454–3458, Dec. 2004.

[32] A. Patel, S. Biswas, and A. K. Jagannatham, "Optimal GLRT-Based Robust Spectrum Sensing for MIMO Cognitive Radio Networks With CSI Uncertainty," *IEEE Trans. Signal Process.*, vol. 64, no. 6, pp. 1621–1633, Mar. 2016.

[33] S. Boyd and L. Vandenberghe, *Convex Optimization*. New York, NY, USA: Cambridge University Press, 2004.

[34] S. M. Kay, *Fundamentals of Statistical Signal Processing, Volume 2: Detection Theory*. New Jersey: Prentice-Hall Inc, 1993.

[35] A. Chawla, A. Patel, A. K. Jagannatham, and P. K. Varshney, "Technical Report: Distributed detection in massive MIMO wireless sensor networks under perfect and imperfect CSI," IIT Kanpur, Tech. Rep., 2019, [Online]. Available: http://www.iitk.ac.in/mwn/documents/TR_DD_MMIMO_2019.pdf.

[36] M. Grant and S. Boyd, "CVX: Matlab software for disciplined convex programming, version 2.1," http://cvxr.com/cvx, Mar. 2014.